

1998

Comparison of median indicator kriging with full indicator kriging in the analysis of spatial data

Donna Hill
Edith Cowan University

Follow this and additional works at: https://ro.ecu.edu.au/theses_hons



Part of the [Geology Commons](#), and the [Statistical Theory Commons](#)

Recommended Citation

Hill, D. (1998). *Comparison of median indicator kriging with full indicator kriging in the analysis of spatial data*. Edith Cowan University. https://ro.ecu.edu.au/theses_hons/462

This Thesis is posted at Research Online.
https://ro.ecu.edu.au/theses_hons/462

Edith Cowan University

Copyright Warning

You may print or download ONE copy of this document for the purpose of your own research or study.

The University does not authorize you to copy, communicate or otherwise make available electronically to any other person any copyright material contained on this site.

You are reminded of the following:

- Copyright owners are entitled to take legal action against persons who infringe their copyright.
- A reproduction of material that is protected by copyright may be a copyright infringement. Where the reproduction of such material is done without attribution of authorship, with false attribution of authorship or the authorship is treated in a derogatory manner, this may be a breach of the author's moral rights contained in Part IX of the Copyright Act 1968 (Cth).
- Courts have the power to impose a wide range of civil and criminal sanctions for infringement of copyright, infringement of moral rights and other offences under the Copyright Act 1968 (Cth). Higher penalties may apply, and higher damages may be awarded, for offences and infringements involving the conversion of material into digital or electronic form.

**Comparison of Median Indicator Kriging with Full Indicator
Kriging in the Analysis of Spatial Data**

**A Thesis Submitted to the
Faculty of Communications, Health and Science
Edith Cowan University
Perth, Western Australia**

by Donna Hill

**In Partial Fulfillment of the Requirements for the Degree
of**

Bachelor of Science Honours (Mathematics)

November 1998

Student Number: XXXXXXXXXX
Supervisors: **Dr Lyn Bloom**
Dr Ute Mueller

USE OF THESIS

The Use of Thesis statement is not included in this version of the thesis.

ABSTRACT

In the earth sciences, and particularly in the mining of precious metals, data distributions are often strongly positively skewed. When making decisions on the potential profitability of a gold mine, for example, the high values of the distribution are of particular importance. Indicator kriging provides estimates of cumulative distribution functions from which grade tonnage curves may be calculated. Multiple or full indicator kriging requires a semivariogram to be modelled and a kriging system of equations to be solved for each cut off. This can be time consuming and modelling indicator semivariograms at high cut-offs may be difficult because of the low number of data above the cut off. One way to avoid these problems is to use median indicator kriging. Median indicator kriging uses the same semivariogram model at each cut off and may not perform as well as full indicator kriging.

This thesis presents comparisons of median indicator kriging and full indicator kriging in the analysis of three suites of data for which the assumptions of median indicator kriging are only approximately satisfied. The distributions of the sample data sets have different degrees of skewness and sparseness. Two of the data suites represent highly skewed gold mineralisations and grade tonnage curves are obtained from the results of both indicator kriging methods. The third suite consists of approximately normally distributed air permeability data. The results from the two methods are compared with reality and show that median indicator kriging performs as well as full indicator kriging in each case.

DECLARATION

I certify that this thesis does not, to the best of my knowledge and belief:

- (i) incorporate without acknowledgement any material previously submitted for a degree or diploma in any institution of higher education;
- (ii) contain any material previously published or written by another person except where due reference is made in the text; or
- (iii) contain any defamatory material.

Signature

Date 12/1/99

ACKNOWLEDGEMENTS

I would like to thank WMC Resources for making the raw data (exploration and blast hole) from the Goodall mine available to ECU. I would also like to thank Danny Kentwell for allowing me to use a subset of his composited data and for making available the code for the bounding polygon used to delimit the irregularly shaped region of the Goodall mine. Thanks go also to my supervisors Dr. Lyn Bloom and Dr. Ute Mueller for their tireless support and encouragement, with an extra thankyou to Dr Ute Mueller for all the cakes and chocolate biscuits she provided along the way.

CONTENTS

Abstract	ii
Declaration	iii
Acknowledgements	iv
 Chapter 1 - Introduction	 1
1.1 Background and Significance.....	1
1.2 Thesis Aims.....	4
1.3 Thesis Outline	5
1.4 Software.....	5
1.5 Notation.....	6
 Chapter 2 - Theoretical Framework	 8
2.1 Regionalized Variables and Random Functions	8
2.2 Semivariograms.....	11
2.2.1 Geometric Anisotropy	16
2.2.2 Zonal Anisotropy.....	18
2.3 Simple and Ordinary Kriging.....	19
2.4 Indicator Kriging	21
2.5 Grade Tonnage Curves.....	26
 Chapter 3 - Data Analysis	 30
3.1 <i>Goodall</i> Data Suite.....	31
3.1.1 Data Sets.....	31
3.1.2 Variography.....	35
3.1.3 Results	38
3.1.4 Order Relation Deviations.....	42
3.1.5 Grade Tonnage Curves.....	42
3.2 <i>True</i> Data Suite.....	44
3.2.1 Data Sets.....	44
3.2.2 Variography.....	46
3.2.3 Results	50
3.2.4 Order Relation Deviations.....	55

3.2.5 Grade Tonnage Curves.....	56
3.3 <i>Berea</i> Data Suite.....	61
3.3.1 Data Sets.....	61
3.3.2 Variography.....	62
3.3.3 Results	69
3.3.4 Order Relation Deviations.....	74
Chapter 4 – Discussion and Conclusions	75
4.1 Discussion	76
4.1.1 Order Relation Deviations.....	77
4.2 Conclusions	79
References	81
Appendix A – Sample Data Sets	83
Appendix B – Estimation of Average Grade Above the Highest Cutoff.....	86
Appendix C – GRADETON Fortran 77 code	89
Appendix D – Example Parameter Files	93

1. INTRODUCTION

In this chapter the importance and general background of geostatistics are discussed. The aims and outline of the thesis are presented along with the notation used throughout.

1.1 Background and Significance

It is important in the earth sciences to be able to estimate the value of an attribute at a particular location in space. Geostatistical methods are used to produce estimates of attributes over an entire region by interpolating from sample values within the same region. These techniques may be used for purposes as diverse as assessing soil quality (Smith, Halvorson & Papendick, 1993) and earthquake prediction (Carr & Bailey, 1986). A major use of geostatistics is in the mining industry (Guarascio, David & Huijbregts, 1976; David, 1988; Fytas, Chaouai & Lavigne, 1990).

When analysing sample data with standard statistical techniques it is assumed that there is independence between samples, so that the value of a sample is not affected by the values of other samples. However, when dealing with spatial data there is often dependence and if two samples are taken from nearby locations, they are likely to have similar values. For example, if we know that a particular part of a region is contaminated with some pollutant then it is quite likely that a nearby part of the region is also contaminated. Geostatisticians incorporate this dependence when trying to obtain estimates of an attribute at unsampled locations.

There are various ways to measure this spatial correlation. Two in common use are the covariance function and the semivariogram. These provide information on the magnitude of the correlation and the distance over which values are related. A semivariogram model is chosen to fit an experimental semivariogram and then there are several weighted multiple linear regression techniques, known collectively as kriging, available for prediction. The weights are dependent on the data locations and the semivariogram model employed. They are calculated by solving a system of equations known as the kriging system.

Some of the commonly used parametric types of kriging are simple kriging (SK), ordinary kriging (OK) and kriging with a trend model (KT) (Goovaerts, 1997). Multiple and median indicator kriging are two of the non-parametric kriging methods frequently used (Vann & Guibal, 1998).

With these and other kriging methods available the important question arises as to which one should be used. The answer to this question depends on the situation. If the data are approximately normally distributed and all that is required is an expected value at a location then a parametric kriging method, such as OK, can be used. If the distribution is highly skewed OK may be used but will tend to overestimate low values and underestimate high values (Pan & Arik, 1993). This is known as conditional bias. Also, extreme values distort the semivariogram, which makes modelling very difficult (Journel, 1983; Fytas, Chaouai & Lavigne, 1990). Indicator kriging methods are less sensitive to extreme values and should perform better than OK in this case (Fytas, Chaouai & Lavigne, 1990; Buxton, Wells & Diluise, 1997). If an estimate of the

distribution at a location is required, rather than an expected value, then parametric methods cannot be used and indicator methods are needed (Vann & Guibal, 1998).

Even if the decision has been made to use an indicator method there still remains the question of which one to choose. It is not always clear which is the most appropriate method and this thesis will compare two indicator kriging methods in an attempt to answer this question. The two methods to be compared are multiple (or full) indicator kriging and median indicator kriging. In order to avoid confusion when using abbreviations, multiple indicator kriging will be referred to as full indicator kriging and abbreviated to fIK while median indicator kriging will be abbreviated to mIK from here on in this thesis.

Both mIK and fIK involve the kriging of indicators, which are constructed by a simple binary transformation of the sample data. For a given cut off value data are coded zero or one according to whether or not they exceed the cut off. By choosing a sequence of cut offs a sequence of indicator values can be produced for each sample datum. Either SK or OK is then performed on the sample indicators at each cut off to produce an estimate of the cumulative distribution function of the attribute at each location. The difference between the two methods lies in the semivariogram model used for the kriging step (Goovaerts, 1997).

The fIK method requires an indicator semivariogram to be modelled for each cut off and therefore at each location the kriging system of equations must be solved for each cut off. The mIK method is a simplified version of fIK in which the same

semivariogram model is used at each cut off. This common model is usually the semivariogram model for the median cut off. The advantages of mIK are that only a single semivariogram needs to be modelled and that the kriging system needs to be solved only once for each location.

1.2 Thesis Aims

The aim of this thesis is to perform comparisons between median indicator kriging and full indicator kriging to see how much information, if any, is lost by using the more time efficient mIK when the assumption that all semivariograms are proportional is only approximately satisfied.

Three suites of data (*Goodall*, *True* and *Berea*) are analysed, as it is likely that mIK may be adequate for some distributions, but not for others. A brief description of the data sets follows; a more detailed description is included in Chapter 3.

The *Goodall* and *True* data suites represent highly skewed gold mineralisation data, the first consisting of real and the second of simulated data. The *Berea* data suite contains permeability data and has an approximately normal distribution. The sparseness of the exploration data sets varies from suite to suite. In all three cases exhaustive data sets are available and used to provide comparisons between the results obtained and reality.

In a mining context it is important to be able to estimate the recoverable reserves of a deposit. For this purpose grade tonnage curves are calculated rather than simply

producing an estimate of the grade at each location. Predicted grade tonnage curves are therefore compared with actual grade tonnage curves for the two gold mineralisations.

1.3 Thesis Outline

Chapter 2 of the thesis presents the theoretical background of this area of geostatistics and explains the relevant kriging methods. Full indicator kriging is explained and the assumptions necessary for median indicator kriging are given in detail. Chapter 3 presents the three data suites in detail and provides the analysis and results for each suite along with discussion of the results. A review of results and conclusions are given in Chapter 4. A summary of these for the *Goodall* data can be found in Hill, Mueller & Bloom (1998).

1.4 Software

The geostatistical and other software used in the analysis of the data are listed below.

GSLIB (Deutsch & Journel, 1992): the following routines

GAMV3M

IK3D

POSTIK

3PLOT (Kanevski et al, 1998)

VARIOWIN 2.2 (Pannatier, 1996)

MINITAB 12

MICROSOFT EXCEL

1.5 Notation

The following notation is used throughout this thesis and is the same as that of the GSLIB user's manual (Deutsch & Journel, 1998) and Goovaerts (1997).

$F(\mathbf{u}; z)$	cumulative probability distribution function at location \mathbf{u}
$F(\mathbf{u}_1, \mathbf{u}_2; z_1, z_2)$	two point cdf
$F(\mathbf{u}_1, \dots, \mathbf{u}_n; z_1, \dots, z_n)$	multivariate cdf
$[F(\mathbf{u}; z_i)]^r$	estimate of the cdf at location \mathbf{u}
$F(z_k)$	proportion of sample values less than or equal to cut off z_k
$g(h)$	model semivariogram
$\gamma(\mathbf{h})$	semivariogram at lag vector \mathbf{h}
$\hat{\gamma}(\mathbf{h})$	experimental semivariogram at lag \mathbf{h}
$\hat{\gamma}_I(\mathbf{h}; z_k)$	experimental indicator semivariogram at lag vector \mathbf{h} and cut off z_k
h	separation distance
\mathbf{h}	separation vector
$i(\mathbf{u}; z_k)$	indicator value at location \mathbf{u} and cut off z_k
$\lambda_{\alpha}(\mathbf{u})$	kriging weight of the sample value at location \mathbf{u}_{α} when estimating the value at \mathbf{u}
$\lambda_{\alpha}^{SK}(\mathbf{u})$	simple kriging weight of the sample value at location \mathbf{u}_{α} when estimating the value at \mathbf{u}

$\lambda_{\alpha}^{OK}(\mathbf{u})$	ordinary kriging weight of the sample value at location \mathbf{u}_{α} when estimating the value at \mathbf{u}
$m(\mathbf{u})$	expected value of random variable $Z(\mathbf{u})$
$m^{\star}(A; z_k)$	estimated average grade above cut off z_k
$\mu_{OK}(\mathbf{u})$	Lagrange multiplier used for ordinary kriging
n	total number of sample data available
$n(\mathbf{u})$	number of sample data values used to estimate the value at location \mathbf{u}
$N(\mathbf{h})$	number of pairs of sample data values separated by lag vector \mathbf{h}
$q(A; z_k)$	quantity of metal contained in ore with grade above z_k
$q^{\star}(A; z_k)$	estimate of the quantity of metal contained in ore with grade above z_k
$r(A; z_k)$	proportion of the tonnage from region A with grade higher than z_k
$T^{\star}(z_k)$	estimated tonnage above the cut off z_k
z_k	k^{th} cut off value for attribute z
\bar{z}_k	average grade between the k^{th} and $(k + 1)^{\text{st}}$ cut offs
$z(\mathbf{u})$	actual attribute value at the unsampled location \mathbf{u}
$z(\mathbf{u}_{\alpha})$	sample attribute value at location \mathbf{u}_{α}
$Z(\mathbf{u})$	random variable at location \mathbf{u}
$Z^{\star}(\mathbf{u})$	kriging estimator of $Z(\mathbf{u})$
$Z_{SK}^{\star}(\mathbf{u})$	simple kriging estimator of $Z(\mathbf{u})$
$Z_{OK}^{\star}(\mathbf{u})$	ordinary kriging estimator of $Z(\mathbf{u})$

2. THEORETICAL FRAMEWORK

In this chapter the theory of regionalised variables is presented briefly followed by a description of semivariograms and kriging. Both FIK and mIK are explained along with the methods used for analysing the results.

2.1 Regionalised Variables and Random Functions

An attribute distributed over a region A in space has, at each location u in A , an associated random variable $Z(u)$. If the attribute being measured was gold grade then at a location u the grade would be a single realisation $z(u)$ from the random variable. The value of the attribute at a particular location is not independent of values at other locations and the single realisation $z(u)$ is known as a regionalised value.

If one sample is taken from each location within A then the set of all these samples is known as a regionalised variable

$$z(u) = \{ z(u_\alpha) \mid \forall u_\alpha \in A \}$$

A regionalised variable is a function describing an attribute over space and exhibits dependence between realisations at different locations (Davis, 1986). Examples of regionalised variables are functions describing ore grades throughout an orebody or pollution levels over a contaminated site.

Using another sampling method would result in a different set of realisations and hence a different regionalised variable $z_1(u)$. The set of all possible regionalised variables on

A is known as a random function

$$Z(\mathbf{u}) = \{ z(\mathbf{u}) \mid \forall \mathbf{u} \in A \}$$

The random function can also be defined as the set of all random variables within A

$$Z(\mathbf{u}) = \{ Z(\mathbf{u}_\alpha) \mid \forall \mathbf{u}_\alpha \in A \}$$

A random function describes the dependence between the different random variables in a probabilistic manner (Isaaks & Srivastava, 1989). An example of a very simple random function is given below in Figure 2.1.

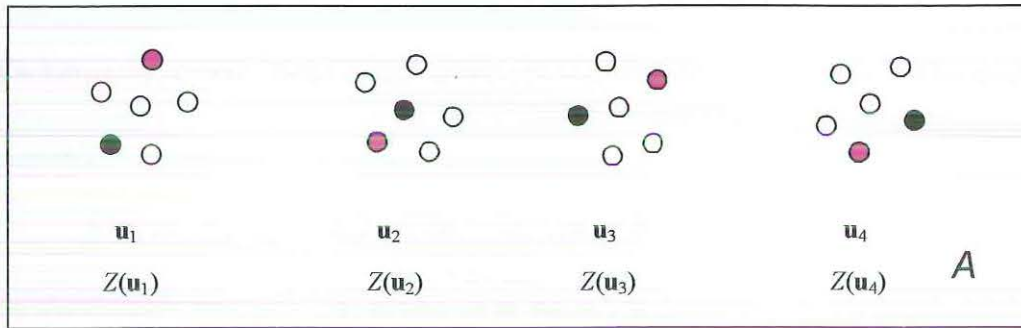


Figure 2.1. A random function.

There are only four locations \mathbf{u}_α , $\alpha = 1, \dots, 4$ within the region A . The random variables $Z(\mathbf{u}_\alpha)$, $\alpha = 1, \dots, 4$ each have six possible outcomes represented by six circles and the pink circle at each location \mathbf{u}_α represents one regionalised value $z_1(\mathbf{u}_\alpha)$. The set of pink circles corresponds to a regionalised variable $z_1(\mathbf{u})$. The black circles show another possible regionalised value $z_2(\mathbf{u}_\alpha)$ for each location \mathbf{u}_α and the set of black circles represents a second possible regionalised variable $z_2(\mathbf{u})$. The random function is the set of all possible regionalised variables or all random variables.

Associated with the attribute of interest at each location \mathbf{u} is a cumulative distribution function (cdf) F defined by

$$F(\mathbf{u}; z) = P(Z(\mathbf{u}) < z)$$

This is the probability that the attribute value at the location \mathbf{u} is less than a specific value z . A two point cdf is defined as the joint probability that the value of the attribute at one location is less than a specific value z_1 , while at the same time the value at a second location is less than a second specific value z_2 . This joint cdf is denoted by

$$F(\mathbf{u}_1, \mathbf{u}_2; z_1, z_2) = P(Z(\mathbf{u}_1) < z_1, P(Z(\mathbf{u}_2) < z_2) \quad (2.1)$$

and Equation 2.1 may be extended to a multivariate cdf

$$F(\mathbf{u}_1, \dots, \mathbf{u}_n; z_1, \dots, z_n) = P(Z(\mathbf{u}_1) < z_1, \dots, Z(\mathbf{u}_n) < z_n) \quad (2.2)$$

(Wackernagel, 1995). If the multivariate cdf is invariant under translation by any vector \mathbf{h} , namely

$$F(\mathbf{u}_1, \dots, \mathbf{u}_n; z_1, \dots, z_n) = F(\mathbf{u}_1 + \mathbf{h}, \dots, \mathbf{u}_n + \mathbf{h}; z_1, \dots, z_n)$$

then the random function $Z(\mathbf{u})$ is said to be strictly stationary (Wackernagel, 1995).

The covariance $C(\mathbf{h})$ of a random function is a measure of the relationship between values of the same attribute at locations separated by a vector or lag \mathbf{h} , and is given by

$$C(\mathbf{h}) = E\{Z(\mathbf{u}) Z(\mathbf{u} + \mathbf{h})\} - E\{Z(\mathbf{u})\}E\{Z(\mathbf{u} + \mathbf{h})\} \quad (2.3)$$

If the expected value and the covariance exist and if both are invariant under translation the random function is stationary of order two (Goovaerts, 1997; Wackernagel, 1995).

In other words, the mean remains constant throughout the region and the covariance is a function of the separation vector \mathbf{h} only.

2.2 Semivariograms

There are other measures of the spatial continuity of a random variable apart from the covariance. Two such measures are the correlogram $\rho(\mathbf{h})$ and the semivariogram $\gamma(\mathbf{h})$.

The correlogram is defined as

$$\rho(\mathbf{h}) = \frac{C(\mathbf{h})}{C(0)} \quad (2.4)$$

where $C(0)$ is the covariance at lag zero which is equal to the variance.

If the random function increments $[Z(\mathbf{u}) - Z(\mathbf{u} + \mathbf{h})]$ are stationary of order two then

$$E\{Z(\mathbf{u} + \mathbf{h}) - Z(\mathbf{u})\} = 0$$

and
$$\text{Var}\{Z(\mathbf{u} + \mathbf{h}) - Z(\mathbf{u})\} = 2\gamma(\mathbf{h}) \quad (2.5)$$

where $\gamma(\mathbf{h})$ is the semivariogram. The assumption of second order stationarity of the increments is known as the intrinsic hypothesis (Journel & Huijbregts, 1978; Goovaerts, 1997). Second order stationarity implies intrinsic stationarity but the converse is not true. An example of a random process which is intrinsically stationary but not second order stationary is Brownian motion (Cressie, 1991).

The correlogram is a standardised form of the covariance and when all three measures exist the following relationships hold

$$\gamma(\mathbf{h}) = C(0) - C(\mathbf{h}) \quad (2.6)$$

and
$$\gamma(\mathbf{h}) = C(0) (1 - \rho(\mathbf{h})) \quad (2.7)$$

The experimental semivariogram at lag \mathbf{h} is defined by

$$\hat{\gamma}(\mathbf{h}) = \frac{1}{2N(\mathbf{h})} \sum_{\alpha=1}^{N(\mathbf{h})} [z(\mathbf{u}_{\alpha}) - z(\mathbf{u}_{\alpha} + \mathbf{h})]^2 \quad (2.8)$$

where $N(\mathbf{h})$ is the number of pairs separated by \mathbf{h} . In order to describe the spatial continuity of the attribute experimental semivariogram values are calculated at various lags in several directions and a model is fitted. Because it is likely that there are few points separated exactly by the given vector \mathbf{h} , tolerances are included when calculating experimental semivariogram values. The calculation is then performed for all pairs separated by distances between $(h + \Delta h)$ and $(h - \Delta h)$ at angles between $(\theta + \Delta \theta)$ and $(\theta - \Delta \theta)$.

The variance of any linear combination of random variables must be non-negative and under the assumption of second order stationarity can be expressed as a sum of covariance values (Journel & Huijbregts, 1978). If the random variable is given by

$$Y = \sum_{\alpha=1}^n \lambda_{\alpha} Z(\mathbf{u}_{\alpha}),$$

then

$$\begin{aligned} \text{Var}\{Y\} &= \text{Var}\left\{\sum_{\alpha=1}^n \lambda_{\alpha} Z(\mathbf{u}_{\alpha})\right\} \\ &= \text{Cov}\{\lambda_1 Z(\mathbf{u}_1) + \dots + \lambda_n Z(\mathbf{u}_n), \lambda_1 Z(\mathbf{u}_1) + \dots + \lambda_n Z(\mathbf{u}_n)\} \\ &= \lambda_1 \sum_{\beta=1}^n \lambda_{\beta} \text{Cov}\{Z(\mathbf{u}_1), Z(\mathbf{u}_{\beta})\} + \dots + \lambda_n \sum_{\beta=1}^n \lambda_{\beta} \text{Cov}\{Z(\mathbf{u}_n), Z(\mathbf{u}_{\beta})\} \\ &= \sum_{\alpha=1}^n \sum_{\beta=1}^n \lambda_{\alpha} \lambda_{\beta} \text{Cov}\{Z(\mathbf{u}_{\alpha}), Z(\mathbf{u}_{\beta})\} \\ &= \sum_{\alpha=1}^n \sum_{\beta=1}^n \lambda_{\alpha} \lambda_{\beta} C(\mathbf{u}_{\alpha} - \mathbf{u}_{\beta}) \\ &= \sum_{\alpha=1}^n \sum_{\beta=1}^n \lambda_{\alpha} \lambda_{\beta} [C(0) - \gamma(\mathbf{u}_{\alpha} - \mathbf{u}_{\beta})] \end{aligned} \tag{2.9}$$

$$= C(0) \sum_{\alpha=1}^n \lambda_{\alpha} \sum_{\beta=1}^n \lambda_{\beta} - \sum_{\alpha=1}^n \sum_{\beta=1}^n \lambda_{\alpha} \lambda_{\beta} \gamma(\mathbf{u}_{\alpha} - \mathbf{u}_{\beta}) \geq 0 \quad (2.10)$$

Equation 2.9 means that the covariance matrix must be positive definite to ensure non-negativity of the variance. As second order stationarity implies intrinsic stationarity it is always possible to derive a semivariogram model from a given covariance model using Equation 2.6. However, the converse is not true and some semivariogram models that are permissible are not bounded above and a corresponding covariance model cannot be obtained. If only intrinsic stationarity is assumed the condition that the weights λ_{α} sum to zero

$$\sum_{\alpha=1}^n \lambda_{\alpha} = 0 \quad (2.11)$$

removes the covariance term from Equation 2.10. This then becomes

$$\text{Var}\{Y\} = - \sum_{\alpha=1}^n \sum_{\beta=1}^n \lambda_{\alpha} \lambda_{\beta} \gamma(\mathbf{u}_{\alpha} - \mathbf{u}_{\beta}) \geq 0 \quad (2.12)$$

The semivariogram model must therefore be conditionally negative definite with the condition being Equation 2.11 (Goovaerts, 1997). If a semivariogram model has a covariance counterpart then conditional negative definiteness of the model is a sufficient but not necessary condition for a non-negative variance. Linear combinations of five basic models are commonly used to ensure that the variance is non-negative. Four of these are bounded above and have a covariance counterpart while the fifth is unbounded and does not have a covariance counterpart.

The four bounded models are the nugget effect, spherical, exponential and Gaussian models and the unbounded model is the power model. The nugget effect and spherical

models reach a maximum value known as the **sill**, whereas the exponential and Gaussian models approach a horizontal asymptote, also called the sill. The range a of the spherical model is the distance at which the sill is reached, while the effective range a of the exponential and Gaussian models is the distance at which 95% of the sill is reached. (Goovaerts, 1997). If the experimental semivariogram is dependent on distance only it is called isotropic, otherwise it is said to be anisotropic. The five basic models, given below in their isotropic form with sill standardised to one are

- Nugget effect model

$$g(h) = \begin{cases} 0 & \text{if } h = 0 \\ 1 & \text{if } h > 0 \end{cases} \quad (2.13)$$

- Spherical model

$$g(h) = \begin{cases} 1.5 \frac{h}{a} - 0.5 \left(\frac{h}{a} \right)^3 & \text{if } h \leq a \\ 1 & \text{if } h > a \end{cases} \quad (2.14)$$

- Exponential model

$$g(h) = 1 - \exp\left(\frac{-3h}{a}\right), \quad h \geq 0 \quad (2.15)$$

- Gaussian model

$$g(h) = 1 - \exp\left(\frac{-3h^2}{a^2}\right), \quad h \geq 0 \quad (2.16)$$

- Power model

$$g(h) = h^\omega \quad \text{with } 0 < \omega < 2, h \geq 0 \quad (2.17)$$

Figure 2.2.1 shows the spherical, exponential and Gaussian semivariogram models.

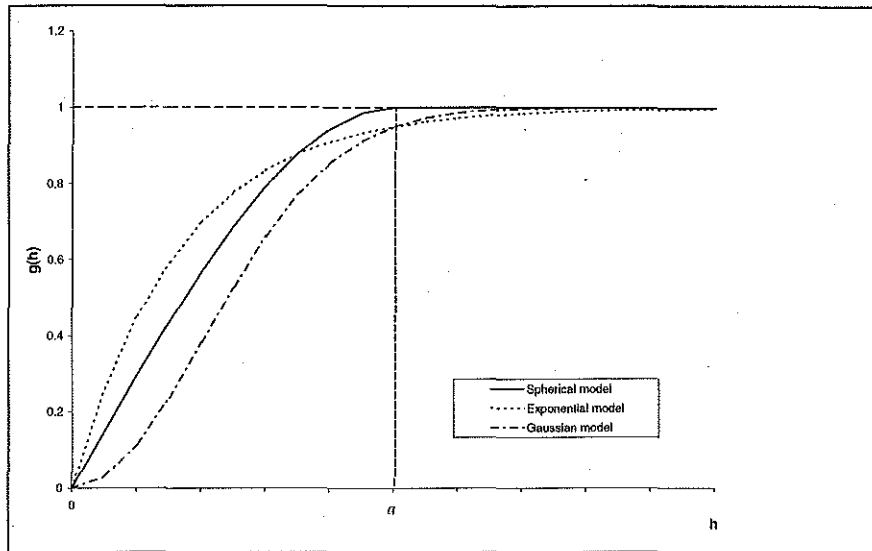


Figure 2.2.1. Three semivariogram models. The dashed vertical line indicates the range of the spherical model and the effective range of the exponential and Gaussian models, respectively. The dashed horizontal line indicates the sill.

The behaviour of the power model is governed by the value of the parameter ω . Three power models with different values of ω are shown in Figure 2.2.2.

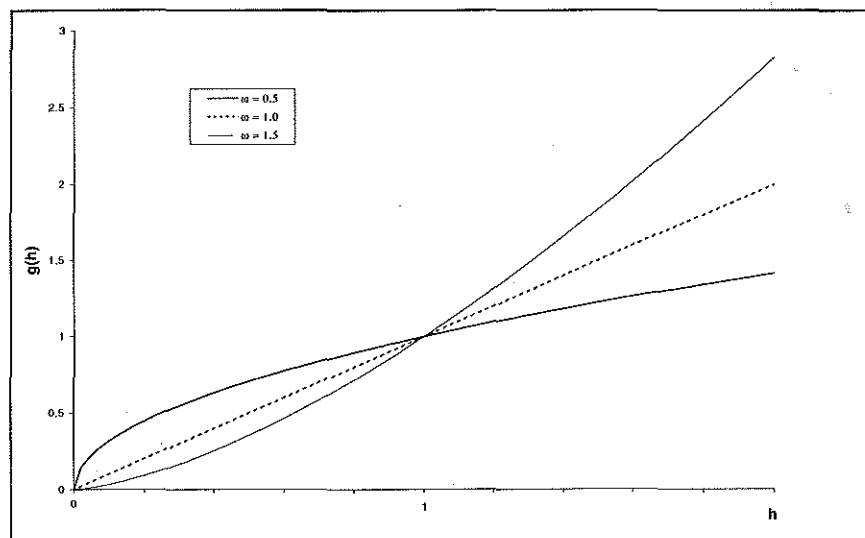


Figure 2.2.2. Power model with three values for ω .

Attributes often exhibit anisotropy or greater continuity in a particular direction, for example dust concentrations in the direction of the prevailing winds or gold grades along a vein. In these cases an isotropic model is inadequate to describe the spatial continuity of the attribute and an anisotropic model needs to be fitted.

Anisotropy may be detected if experimental semivariograms are calculated separately in different directions. If the directional semivariograms have the same shape and sill but the ranges vary smoothly, so that a plot of range versus direction produces an ellipse (see Figure 2.2.3), the anisotropy is said to be geometric. If the directional semivariograms have different sills the anisotropy is said to be zonal (Goovaerts, 1997).

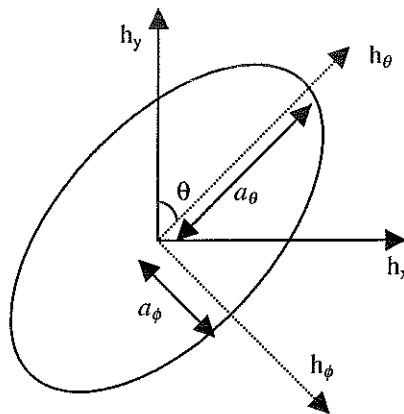


Figure 2.2.3. The ellipse shows the range in different directions. Maximum and minimum ranges are a_θ and a_ϕ respectively.

2.2.1 Geometric Anisotropy

An example of geometric isotropy is given in Figure 2.2.4 showing the directions of maximum and minimum continuity. In order to use an isotropic semivariogram model

the ellipse may be transformed into a circle via a principal axis transformation. If the directions of maximum and minimum continuity are at angles θ and ϕ from the vertical axis respectively (with $\phi - \theta = 90^\circ$) and the corresponding ranges are a_θ and a_ϕ then the vector $\mathbf{h} = (h_x, h_y)^T$ may be transformed to a new vector $\mathbf{h}' = (h_\phi, h_\theta)^T$ by a rotation through the angle θ followed by a contraction by a factor $\lambda = a_\phi / a_\theta$

$$\mathbf{h}' = \begin{bmatrix} h_\phi \\ h_\theta \end{bmatrix} = \begin{bmatrix} 1 & 0 \\ 0 & \lambda \end{bmatrix} \begin{bmatrix} \cos \theta & -\sin \theta \\ \sin \theta & \cos \theta \end{bmatrix} \begin{bmatrix} h_x \\ h_y \end{bmatrix} \quad (2.18)$$

The anisotropic model may now be replaced with an isotropic model

$$g_a(\mathbf{h}) = g_i(h') \quad (2.19)$$

where the subscripts a and i refer to anisotropic and isotropic models respectively, and the isotropic model has range a_ϕ .

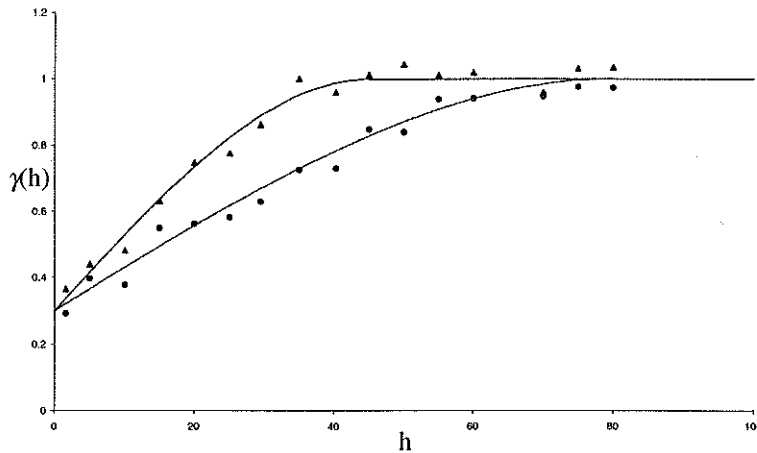


Figure 2.2.4. An example of purely geometric anisotropy. The lower curve has a larger range and corresponds to the direction of maximum continuity and the upper curve with shorter range corresponds to the direction of minimum continuity.

2.2.2 Zonal Anisotropy

If the sill of the experimental semivariogram varies with direction the anisotropy is said to be zonal. With a zonal model the direction with the lowest sill is the direction of maximum continuity and perpendicular to it is the direction of minimum continuity which has the highest sill (see Figure 2.2.5). First an isotropic model is fitted to match the lowest sill. Then the sill is increased in the direction of minimum continuity while it is kept constant in the direction of maximum continuity. This is accomplished by adding a model with geometric anisotropy which has an infinite range in the direction of maximum continuity. This is equivalent to setting the factor λ , from Equation 2.18, to zero.

The zonal model is

$$g(\mathbf{h}) = g_1(h) + g_2(\mathbf{h}) \quad (2.20)$$

where $g_1(h)$ is an isotropic model with range a_ϕ and $g_2(\mathbf{h})$ is an anisotropic model with infinite range a_θ and finite range a_ϕ .

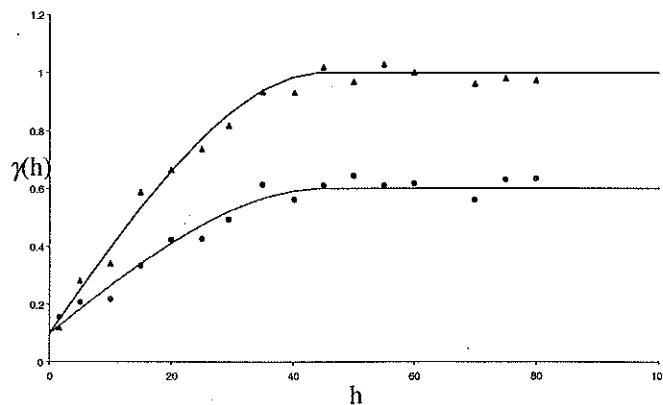


Figure 2.2.5. An example of purely zonal anisotropy. The two directional semivariograms have the same range but different sills. The lower sill corresponds to the direction of maximum continuity and the higher sill corresponds to the direction of minimum continuity.

2.3 Simple and Ordinary Kriging

Once a model has been found for the spatial continuity of an attribute over a region it can be used to estimate values at unsampled locations. The estimator used in kriging is $Z^*(\mathbf{u})$ which is defined as

$$Z^*(\mathbf{u}) = m(\mathbf{u}) + \sum_{\alpha=1}^{n(\mathbf{u})} \lambda_{\alpha}(\mathbf{u}) [Z(\mathbf{u}_{\alpha}) - m(\mathbf{u}_{\alpha})] \quad (2.21)$$

where $m(\mathbf{u})$ and $m(\mathbf{u}_{\alpha})$ are the expected values of the random variables $Z(\mathbf{u})$ and $Z(\mathbf{u}_{\alpha})$ respectively and $\lambda_{\alpha}(\mathbf{u})$ is the weight given to the sample value at position \mathbf{u}_{α} . The number of data used for estimation at each point, $n(\mathbf{u})$, will not necessarily remain constant and will usually be less than n , the total number of sample points. The weights are chosen so as to minimise the estimation variance while remaining unbiased. (Goovaerts, 1997). The derivations of the simple and ordinary kriging systems are outlined below. For full derivations see Goovaerts (1997) or Isaaks and Srivastava (1989).

With simple kriging the mean is assumed known and constant throughout the region and Equation 2.21 becomes

$$\begin{aligned} Z_{SK}^*(\mathbf{u}) &= m + \sum_{\alpha=1}^{n(\mathbf{u})} \lambda_{\alpha}^{SK}(\mathbf{u}) [Z(\mathbf{u}_{\alpha}) - m] \\ &= \sum_{\alpha=1}^{n(\mathbf{u})} \lambda_{\alpha}^{SK}(\mathbf{u}) Z(\mathbf{u}_{\alpha}) + \left[1 - \sum_{\alpha=1}^{n(\mathbf{u})} \lambda_{\alpha}^{SK}(\mathbf{u}) \right] m \end{aligned} \quad (2.22)$$

The estimation error variance, $\sigma_E^2(\mathbf{u}) = \text{Var}\{Z_{SK}^*(\mathbf{u}) - Z(\mathbf{u})\}$, may be expressed in terms of kriging weights and covariances as

$$\sigma_E^2(\mathbf{u}) = \sum_{\alpha=1}^{n(\mathbf{u})} \sum_{\beta=1}^{n(\mathbf{u})} \lambda_{\alpha}^{SK}(\mathbf{u}) \lambda_{\beta}^{SK}(\mathbf{u}) C(\mathbf{u}_{\alpha} - \mathbf{u}_{\beta}) + C(0) - 2 \sum_{\alpha=1}^{n(\mathbf{u})} \lambda_{\alpha}^{SK}(\mathbf{u}) C(\mathbf{u}_{\alpha} - \mathbf{u}) \quad (2.23)$$

where $C(\mathbf{u}_{\alpha} - \mathbf{u}_{\beta})$ is the covariance of $Z(\mathbf{u}_{\alpha})$ with $Z(\mathbf{u}_{\beta})$. The optimal kriging weights are found by setting the partial derivatives of the error variance with respect to the kriging weights equal to zero. The first and second partial derivatives are given by

$$\frac{\partial}{\partial \lambda_{\alpha}^{SK}} (\sigma_E^2(\mathbf{u})) = 2 \sum_{\beta=1}^{n(\mathbf{u})} \lambda_{\beta}^{SK} C(\mathbf{u}_{\alpha} - \mathbf{u}_{\beta}) - 2C(\mathbf{u}_{\alpha} - \mathbf{u}) \quad \text{for } 1 \leq \alpha \leq n(\mathbf{u}) \quad (2.24)$$

and
$$\frac{\partial^2}{\partial \lambda_{\alpha}^{SK} \partial \lambda_{\beta}^{SK}} (\sigma_E^2(\mathbf{u})) = 2C(\mathbf{u}_{\alpha} - \mathbf{u}_{\beta}) \quad \text{for } 1 \leq \alpha, \beta \leq n(\mathbf{u}) \quad (2.25)$$

respectively. The matrix of second partial derivatives in this case is twice the covariance matrix which we know to be positive definite. Hence setting the first partial derivatives to zero will locate the minimum. A straightforward rearrangement of Equation 2.24 then leads to the simple kriging system

$$\sum_{\beta=1}^{n(\mathbf{u})} \lambda_{\beta}^{SK}(\mathbf{u}) C(\mathbf{u}_{\alpha} - \mathbf{u}_{\beta}) = C(\mathbf{u}_{\alpha} - \mathbf{u}) \quad \text{for } \alpha = 1, \dots, n(\mathbf{u}) \quad (2.26)$$

For ordinary kriging the (unknown) mean is assumed constant only in a local neighbourhood of the given point rather than throughout the region. The mean is then filtered from the estimator of Equation 2.21 via the additional condition that the sum of the kriging weights must be one.

$$\begin{aligned} Z_{OK}^*(\mathbf{u}) &= \sum_{\alpha=1}^{n(\mathbf{u})} \lambda_{\alpha}^{OK}(\mathbf{u}) Z(\mathbf{u}_{\alpha}) + \left[1 - \sum_{\alpha=1}^{n(\mathbf{u})} \lambda_{\alpha}^{OK}(\mathbf{u}) \right] m(\mathbf{u}) \\ &= \sum_{\alpha=1}^{n(\mathbf{u})} \lambda_{\alpha}^{OK}(\mathbf{u}) Z(\mathbf{u}_{\alpha}) \quad \text{with} \quad \sum_{\alpha=1}^{n(\mathbf{u})} \lambda_{\alpha}^{OK}(\mathbf{u}) = 1 \end{aligned} \quad (2.27)$$

The minimum error variance is found by using the method of Lagrange multipliers. The following system of $n(\mathbf{u}) + 1$ equations is obtained

$$\begin{cases} \sum_{\beta=1}^{n(u)} \lambda_{\beta}^{OK} C(u_{\alpha} - u_{\beta}) + \mu_{OK}(u) = C(u_{\alpha} - u) & \text{for } \alpha = 1, \dots, n(u) \\ \sum_{\beta=1}^{n(u)} \lambda_{\beta}^{OK}(u) = 1 \end{cases} \quad (2.28)$$

Remembering that $\gamma(h) = C(0) - C(h)$, the ordinary kriging system (2.28) may also be expressed in terms of the semivariogram

$$\begin{cases} \sum_{\beta=1}^{n(u)} \lambda_{\beta}^{OK}(u) \gamma(u_{\alpha} - u_{\beta}) - \mu_{OK}(u) = \gamma(u_{\alpha} - u) & \text{for } \alpha = 1, \dots, n(u) \\ \sum_{\beta=1}^{n(u)} \lambda_{\beta}^{OK}(u) = 1 \end{cases} \quad (2.29)$$

2.4 Indicator Kriging

Once a cut-off or threshold value is chosen, data can be transformed into an indicator variable based on whether or not the threshold, z_k , is exceeded. The value of a sample taken at position u_{α} is denoted by $z(u_{\alpha})$. Then the indicator variable is defined as

$$i(u_{\alpha}; z_k) = \begin{cases} 1, & \text{if } z(u_{\alpha}) \leq z_k \\ 0, & \text{otherwise} \end{cases} \quad (2.30)$$

(Goovaerts, 1997).

A series of indicator thresholds may be used to produce an approximation of the cdf for the attribute at each location. The proportion of sample values below z_k is equal to the average value of the indicators for the cut-off z_k

$$F(z_k) = \frac{1}{n} \sum_{\alpha=1}^n i(u_{\alpha}; z_k) \quad (2.31)$$

where n is the number of sample data points (Isaaks & Srivastava, 1989). This provides a naive estimate for the global cdf without taking into account any spatial continuity, similar to estimating the global mean by simply taking the sample average. In order to make use of spatial continuity either SK or OK may be performed on the indicators of the sample data and this is called indicator kriging.

Experimental indicator semivariograms are relatively unaffected by the presence of outliers, for most cut-offs, as they count pairs which fall on opposite sides of a threshold without taking into account the magnitude of the difference between the pairs. Outliers are therefore not as significant as when calculating ordinary semivariograms. The experimental indicator semivariogram is given by

$$\hat{\gamma}_I(\mathbf{h}; z_k) = \frac{1}{2N(\mathbf{h})} \sum_{\alpha=1}^{N(\mathbf{h})} [i(\mathbf{u}_\alpha; z_k) - i(\mathbf{u}_\alpha + \mathbf{h}; z_k)]^2 \quad (2.32)$$

where $N(\mathbf{h})$ is the number of pairs separated by the vector \mathbf{h} . (Goovaerts, 1997). At very high cut-offs (for example the 99th percentile) there will be few samples with indicator value zero. Because of this the number of pairs which actually contribute to the semivariogram will be small. Consequently, semivariograms at upper thresholds may be poorly behaved and difficult to model (Fytas, Chaouai & Lavigne, 1990).

IK is not used to provide point estimates of actual values but to provide estimates of cumulative probability distributions. This enables one to estimate the probability of exceeding a critical value at a particular location. (Journel, 1988). The critical value depends on the situation and may be a grade above which mining would be profitable, or it may be a legal maximum concentration of some pollutant.

Full indicator kriging involves kriging the indicators at each threshold. The indicator semivariograms must be modelled at each cut-off and a system of equations must be solved at each cut-off and location to provide kriging weights. The system of equations is either the SK system of Equation 2.26 or the OK system of Equation 2.28 with the only difference being that the covariance or semivariogram used is that of the indicators.

The mIK algorithm assumes that the K indicator random functions are intrinsically correlated which means that the indicator semivariogram models are all proportional to a common model. Thus all semivariogram models may be obtained by rescaling a common model $\gamma_m(\mathbf{h})$

$$\gamma(\mathbf{h}; z_k) = \varphi_k \gamma_m(\mathbf{h}) \quad \forall k \quad (2.33)$$

where $\gamma(\mathbf{h}; z_k)$ is the indicator semivariogram model at cut off z_k (Goovaerts, 1997).

The same semivariogram model may be used at each cut off and the procedure is much less demanding computationally. Since a common model is used, the kriging system is the same at each cut off and so only needs to be solved once for each location. The resulting weights at the location are then used for each cut off.

The common semivariogram model is usually chosen to be the model for the semivariogram at a cut-off close to the median value (Goovaerts, 1997). At the median cut-off 50% of samples will have an indicator value of one and 50% an indicator value of zero. Thus the number of pairs that contribute to the experimental semivariogram at

this cut-off is large and the semivariogram is likely to be well behaved and reasonably easy to model (Isaaks & Srivastava, 1989).

In order for the indicator kriging estimates to provide a valid estimation of a cdf certain order relations must be satisfied. All values must lie between zero and one and the estimates must be non-decreasing as the cut off value increases.

$$0 \leq [F(\mathbf{u}; z_k)]^* \leq [F(\mathbf{u}; z_{k+1})]^* \leq 1 \quad \text{for } 1 \leq k \leq K-1 \quad (2.34)$$

There is no inherent reason for the indicator kriging system to produce estimates which automatically satisfy these conditions and usually some estimates do not satisfy the conditions. These order relation deviations may occur for several reasons. As there is no condition that the kriging weights must be non-negative the kriging estimate is a non-convex linear combination of the sample data, which can lead to estimates less than zero or greater than one (Goovaerts, 1994). Also as a different semivariogram model is used at each cut off for fIK, there is no guarantee that the estimates will increase monotonically as the cut offs increase (Goovaerts, 1997).

With mIK the same semivariogram model and hence the same kriging weights are used at each cut off and the estimates will automatically be non-decreasing. Therefore fewer order relation deviations should be obtained from mIK than fIK. The number of order relation deviations may increase when there are no sample data between two consecutive cut offs or when there are sudden changes in the model between cut offs (Deutsch and Journel, 1998).

Order relation deviations must be corrected to obtain a valid cdf. A three-step approach to correct order relation deviations is given in Deutsch and Journel (1998). Step one consists of performing an upward correction. All estimates outside the interval [0, 1] are reset to the nearest bound (i.e. either 0 or 1)

$$[F(\mathbf{u}; z_k)]_U^* = \begin{cases} 0 & \text{if } [F(\mathbf{u}; z_k)]^* < 0 \\ 1 & \text{if } [F(\mathbf{u}; z_k)]^* > 1 \\ [F(\mathbf{u}; z_k)]^* & \text{otherwise} \end{cases}$$

Then starting at the lowest cut off and working upwards any estimate which is lower than the previous one is reset to equal the previous estimate.

Set $[F(\mathbf{u}; z_1)]_U^{**} = [F(\mathbf{u}; z_1)]_U^*$

and for $k = 2$ to K , $[F(\mathbf{u}; z_k)]_U^{**} = \begin{cases} [F(\mathbf{u}; z_k)]_U^* & \text{if } [F(\mathbf{u}; z_k)]_U^* \geq [F(\mathbf{u}; z_{k-1})]_U^{**} \\ [F(\mathbf{u}; z_{k-1})]_U^{**} & \text{otherwise} \end{cases}$

The second step takes a similar approach. Estimates outside the interval [0, 1] are again reset to the nearest bound

$$[F(\mathbf{u}; z_k)]_D^* = \begin{cases} 0 & \text{if } [F(\mathbf{u}; z_k)]^* < 0 \\ 1 & \text{if } [F(\mathbf{u}; z_k)]^* > 1 \\ [F(\mathbf{u}; z_k)]^* & \text{otherwise} \end{cases}$$

and then a downward correction is made by starting at the highest cut off and resetting any estimate that is higher than the previous one to the previous estimate.

Set $[F(\mathbf{u}; z_K)]_D^{**} = [F(\mathbf{u}; z_K)]_D^*$

and for $k = K-1$ to 1 , $[F(\mathbf{u}; z_k)]_D^{**} = \begin{cases} [F(\mathbf{u}; z_k)]_D^* & \text{if } [F(\mathbf{u}; z_k)]_D^* \leq [F(\mathbf{u}; z_{k+1})]_D^{**} \\ [F(\mathbf{u}; z_{k+1})]_D^{**} & \text{otherwise} \end{cases}$

In the third step the upward and downward corrections are averaged to provide the final corrected estimates given in Equation 2.35.

$$[F(u; z_k)]^* = \frac{[F(u; z_k)]_U^* + [F(u; z_k)]_D^*}{2} \quad (2.35)$$

All order relation deviations encountered are corrected automatically by the above method when using the IK3D sub-routine of the GSLIB software (Deutsch and Journel, 1992).

2.5 Grade Tonnage Curves

The aim of geostatistical analysis in the mining industry is to produce an accurate estimate of recoverable resources. This is usually done with grade tonnage curves. For each chosen cut off grade the tonnage of ore in the entire deposit with a grade higher than that cut-off grade is calculated. The average grade of all the ore with grade above the cut off is also determined (Clark, 1979; David, 1988). The tonnage above the cut-off versus the average grade is then graphed for a series of cut-offs, and this graph is called the grade tonnage curve.

In practice a change of support correction needs to be made if point estimates are to be converted to block estimates (Vann & Guibal, 1998; Glacken & Blackney, 1998; Isaaks & Srivastava, 1989). However in this study point estimates are compared with point grade control data without attempting to accurately calculate recoverable resources and so no change of support is used. Each point will be considered to represent a block with centroid on the datum location.

For a cut off z_k the proportion of the total tonnage from within a region A with grade higher than z_k is given by

$$t(A; z_k) = 1 - F(A; z_k) \quad (2.36)$$

where
$$F(A; z_k) = \int_A i(\mathbf{u}, z_k) d\mathbf{u} \quad (2.37)$$

The proportion $F(A; z_k)$ is estimated by summing the indicators at cut off z_k over the region A and dividing by the number of blocks within the region

$$F^*(A; z_k) = \frac{1}{N(A)} \sum_A i^*(\mathbf{u}_a; z_k) \quad (2.38)$$

where $N(A)$ is the number of blocks within A . The estimate for the tonnage of ore in the region A with an average grade above z_k is then the proportion above z_k multiplied by the block size and density. If the region A is the whole deposit then the following formula gives the estimated tonnage above cut off z_k

$$T^*(z_k) = t(A; z_k) N(A) x_b y_b z_b \delta \quad (2.39)$$

where x_b , y_b and z_b are the block dimensions and δ is the density of the ore. Following Journel (1983) we define the quantity of metal recovery factor by

$$q(A; z_k) = \int_{z_k}^{\infty} u dF(A; u)$$

This is estimated by

$$q^*(A; z_k) = \sum_{\alpha=k}^{K-1} \bar{z}_\alpha [F(A; z_{\alpha+1}) - F(A; z_\alpha)] + \bar{z}_K [1 - F(A; z_K)] \quad (2.40)$$

where K is the number of cut offs and \bar{z}_α is the average grade between cut offs z_α and $z_{\alpha+1}$. The value of \bar{z}_α depends on the method of interpolation used to estimate cdf

values between cut offs, and, if linear interpolation is used, its value is given by

$$\bar{z}_\alpha = \frac{z_\alpha + z_{\alpha+1}}{2} \quad (2.41)$$

In the second term on the RHS of Equation 2.40, \bar{z}_k represents the average grade above the highest cut off z_k . This estimate requires extrapolation above the cut off. For positively skewed distributions a hyperbolic model is often used to produce cdf values above z_k . The hyperbolic model is

$$[F(A; z)]_{hyp} = 1 - \frac{\lambda}{z^\omega}, \quad \omega \geq 1, \quad z > z_k \quad (2.42)$$

How quickly the cdf increases to the limit of 1 depends on the value chosen for the exponent ω . The longest tail is produced for $\omega = 1$. The parameter λ in Equation 2.42 is determined from the sample cdf at the highest cut off. It is given by

$$\lambda = \{1 - F^*(A; z_k)\} z_k^\omega \quad (2.43)$$

One cannot simply use Equation 2.42 to provide a maximum possible value of z because $[F(A; z)]_{hyp}$ only approaches 1 asymptotically. A maximum value for either z or $[F(A; z)]_{hyp}$ must be chosen to allow the calculation of an estimate for \bar{z}_k . Gold distributions are very highly skewed and an understanding of the geology of the region is very important if a realistic maximum z value is to be chosen. In this study realistic values are unknown and a maximum value for $[F(A; z)]_{hyp}$, which will be called ϕ_{max} , will be chosen instead.

Once ϕ_{\max} is set the corresponding z value is determined from Equation 2.42

$$z_{\max} = \left(\frac{\lambda}{1 - \phi_{\max}} \right)^{\frac{1}{\omega}} \quad (2.44)$$

where z_{\max} is the maximum grade. This leads to the following estimates for \bar{z}_k .

When $\omega > 1$

$$\bar{z}_k \approx \frac{z_k(1 - F(A; z_k)) - z_{\max}(1 - \phi_{\max}) + \frac{\lambda}{\omega - 1}(z_k^{1-\omega} - z_{\max}^{1-\omega})}{\phi_{\max} - F(A; z_k)} \quad (2.45)$$

When $\omega = 1$

$$\bar{z}_k \approx \frac{z_k(1 - F(A; z_k)) - z_{\max}(1 - \phi_{\max}) + \lambda(\ln(z_{\max}) - \ln(z_k))}{\phi_{\max} - F(A; z_k)} \quad (2.46)$$

The derivations of Equations 2.45 and 2.46 are given in Appendix B. The estimate for the quantity of metal recovery factor may now be determined, using Equation 2.45 or 2.46 with Equation 2.40. The average grade above the k^{th} cut off is then estimated by

$$m^*(A; z_k) = \frac{q^*(A; z_k)}{t(A; z_k)} \quad (2.47)$$

The Fortran routine GRADETON was written to calculate the tonnage and the average grade above each cut off using the above equations and is included in Appendix C. The calculations are made using linear interpolations between cut offs and between the lowest cut off and zero. A hyperbolic extrapolation is used above the highest cut off with values for ω and ϕ_{\max} required as inputs.

3. DATA ANALYSIS

Three suites of data were analysed for the comparison of mIK and fIK (see Table 3.1). Two of the suites, one real and one simulated, represent highly skewed gold mineralisation data. The real gold data come from a region of the Goodall gold mine in the Northern Territory, which was mined by WMC Resources (Kentwell, Bloom & Comber, 1997). The simulated gold data suite is the so-called *True* example data set provided with the GSLIB software (Deutsch & Journel, 1998). The third data suite, the *Berea* data, contains air permeability measurements taken from a slab of Berea sandstone (Journel & Alabert, 1989). Unlike the gold data, the distribution of the *Berea* data is approximately normal.

Each suite of data contains exploration data and exhaustive data. The sparseness of the exploration data sets varies between suites. The exploration set of the *Goodall* data suite is very sparse, that of the *True* data suite is somewhat sparse and that of the *Berea* data suite is not at all sparse. In the case of the *Goodall* data suite there is also an enlarged exploration set which was used for variography. The exhaustive data sets of all three suites represent reality and were used to assess the performance of mIK and fIK. For the purposes of modelling and estimation all data were treated as point data.

Table 3.1. Make-up of the three suites of data

Suite	Data set used for estimation	Data set used for comparison
<i>Goodall</i>	Exploration and variography data sets	Blast hole data set
<i>True</i>	<i>True</i> 97 data set	Exhaustive <i>True</i> data set
<i>Berea</i>	<i>Berea</i> /28 data set	Exhaustive <i>Berea</i> data set

Experimental indicator semivariograms were calculated for different cut off grades. Ten cut off grades were chosen, corresponding to the deciles and the 95th percentile for each data set. Models were fitted to each of these semivariograms for use with FIK, however not all cut offs were used in the final analysis of the *Goodall* data. Standardised semivariograms were used for each data set to try to reduce the occurrence of order relation deviations and hence the need for corrections. Simple kriging of the indicators was used for the *Goodall* data suite due to the sparseness of the sample data and ordinary kriging was used for both the *True* and *Berea* data suites. All order relation deviations were corrected by averaging upward and downward corrections.

E-type estimates were obtained from the estimates of the conditional cumulative distribution functions. These were compared directly with the exhaustive data for each data set. Grade tonnage curves were also calculated from estimates for the *Goodall* and *True* data sets and compared with actual grade tonnage curves.

3.1 Goodall Data Suite

3.1.1 Data Sets

The *Goodall* data come from the Goodall gold mine, which is located in the Northern Territory of Australia, approximately 150km SE of Darwin. The mine falls within the Pine Creek 1:250 000 map sheet, at 8 525 000 mN: 750 000 mE. During open pit operations 4.095 million tonnes of ore were produced at a head grade of 1.99 g/t. Mining was completed in 1992 (Quick, 1994).

The data used in this study are from the A-pod orebody of the main open pit. The part of the orebody analysed is located between mine co-ordinates 10 800 – 11 100N and 10 130 – 10 210E (see Figure 4 in Quick (1994)). Kentwell (1997) carried out all preliminary data processing (combination of drilling data, compositing of blast hole data and of drilling data and construction of the variography data set). The raw drilling data consisted of inclined diamond and RC holes drilled during the exploration stage and these were composited to 2.5m vertical lengths. Summary statistics of the two drilling types showed no substantial differences so all drilling data were combined. In order to perform a two-dimensional analysis only data from a single bench were used.

The *exploration* set contains gold analyses from the composited drilling data taken from within the 540mRL bench. The exhaustive data set consists of gold analyses from the mining stage blast holes drilled into the same bench, which were also composited to represent 2.5m vertical thickness. The composited data were divided into mineralised and non-mineralised populations with a cut off of 0.5 g/t used to define the orebody.

Because the *exploration* data set contains only 21 samples an enlarged subset, referred to as the *variography* data set, containing additional drilling samples from up to 20m above and 20m below the 540mRL bench was used for the variography. The total size of this set is 638 samples. Figure 3.1.1 shows the locations and grades of the *exploration* data set and a plan view of the *variography* data set. The *variography* data set contains data from the region between 10600N and 11300N, but Figure 3.1.1 only shows that located within the same region as the *exploration* data set. The location of

the *exploration* data set in relation to the *variography* data set is shown in Figure 3.1.2.

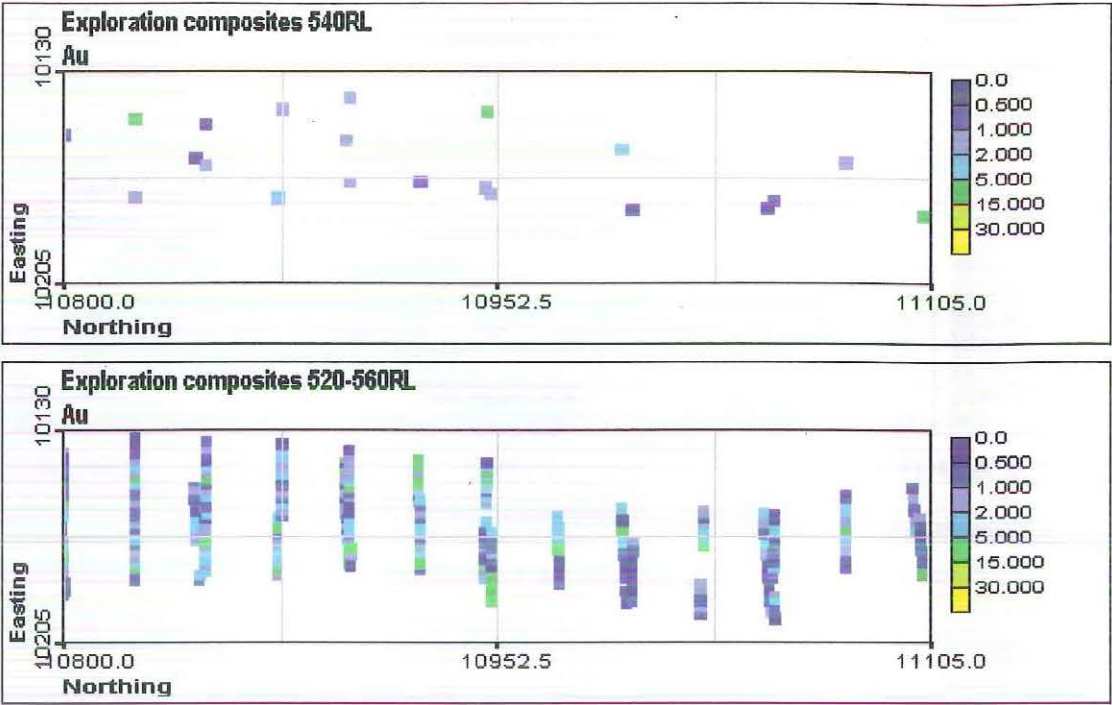


Figure 3.1.1. *Exploration* (top) and *variography* (bottom) data sets for the *Goodall* data suite.

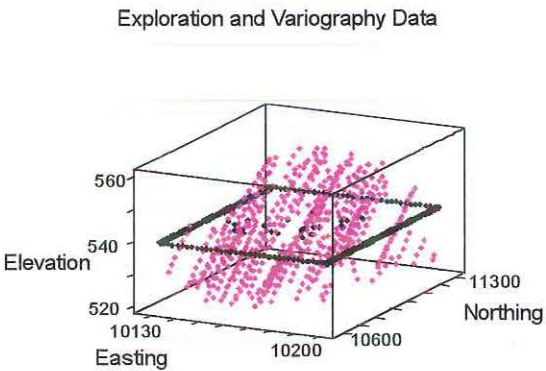


Figure 3.1.2. Locations of *exploration* and *variography* data. Plane indicates 540mRL bench.

Blast holes were drilled on a four metre by two metre grid. The size of the data set was

reduced to 720 samples by removing holes which did not lie on an approximately four metre by four metre grid (Kentwell, Bloom & Comber, 1997). The spatial distribution of grades is shown in Figure 3.1.3.

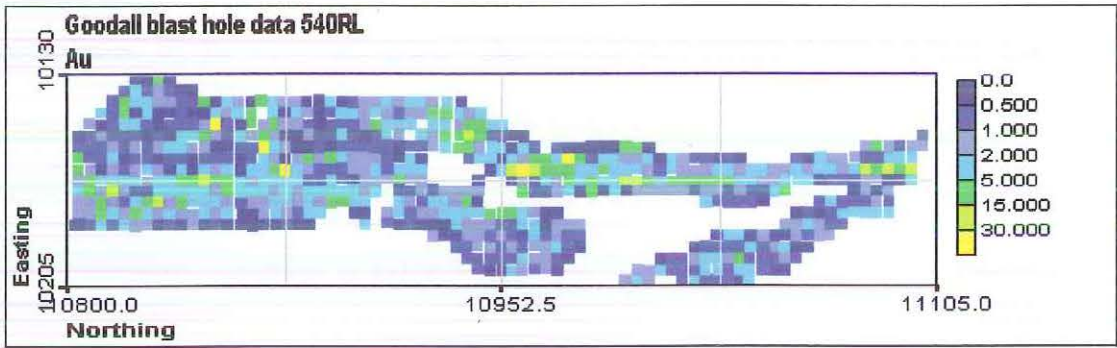


Figure 3.1.3. Blasthole grades.

Summary statistics for the three data sets (see Table 3.1.1) exhibit the highly skewed nature of the distribution. There appears to be some difference between the distribution of the *blasthole* data and the *variography* data. The *variography* data set has lower mean, median and standard deviation than the *blast hole* data set. These differences are not unexpected considering the different spatial extent and sample density of the two data sets. The *exploration* data set also has a lower mean, median and standard deviation than the *blast hole* data and is much less highly skewed.

Table 3.1.1. Summary statistics for the three *Goodall* data sets.

Data set	N	Mean	Median	Standard Deviation	Minimum	Maximum	Skewness
<i>Exploration</i>	21	2.27	1.25	2.92	0.05	12.68	2.57
<i>Variography</i>	638	1.74	0.88	2.53	0.00	25.88	4.00
<i>Blasthole</i>	720	2.77	1.42	4.62	0.01	49.30	4.80

3.1.2 Variography

Since the *exploration* data set is from a single bench and was treated as two-dimensional the vertical bandwidth for calculating the experimental indicator semivariograms from the *variography* set was set to one metre. Thus a pair only contributed to the semivariogram value if the two samples were within one metre vertically of each other. This amounts to looking only at pairs within layers which are essentially two-dimensional. The parameters used in the calculation of the experimental semivariograms are given in Table 3.1.2.

Table 3.1.2: Experimental semivariogram parameters – all distances measured in metres.

Number of lags	10
Lag spacing	10
Lag tolerance	5
Horizontal bandwidth	10
Vertical bandwidth	1
Angular tolerance	30°

The semivariogram value for a lag was discarded if the number of pairs contributing to the semivariogram was less than 15 for that lag. Due to the long narrow shape of the mineralised zone, the experimental semivariograms in the E-W direction were only reliable for the first two or three lags. More emphasis was therefore placed on fitting a model for the N-S direction, which was assumed to be the direction of maximum continuity. Most semivariograms had a similar overall sill for both directions, so it was decided to fit models with purely geometric anisotropy at all cut offs.

Indicator semivariograms were modelled for ten cut offs and standardised by dividing each semivariogram by the total sill, as suggested in Goovaerts (1997). The value at the first lag in the N-S direction was discarded for the 20% and 95% cut offs as it was equal to zero. This means that all closely spaced pairs had grades above the cut off or all below the cut off in each case.

The lack of a reliable semivariogram value at a low lag caused problems with the semivariogram modelling as a variety of models could be used to provide similar fits to the values at higher lags. In particular the choice of nugget value was quite open. A single spherical structure plus nugget was fitted in each case. Table 3.1.3 shows the standardised semivariogram model parameters for the ten cut offs.

Table 3.1.3: Standardised semivariogram model parameters for the *Goodall* data.

Cut off		Semivariogram parameters – spherical model plus nugget				
Percentage	Grade	Nugget	Partial sill	Maximum range	Minimum range	Anisotropy factor
10	0.14	0.30	0.70	45	27	0.600
20	0.30	0.50	0.50	40	20	0.500
30	0.47	0.50	0.50	30	13	0.433
40	0.66	0.40	0.60	35	12	0.343
50	0.88	0.25	0.75	35	10	0.286
60	1.23	0.50	0.50	40	15	0.375
70	1.65	0.50	0.50	30	15	0.500
80	2.39	0.40	0.60	45	30	0.667
90	4.30	0.55	0.45	45	35	0.778
95	6.05	0.25	0.75	45	30	0.667

Because of the sparseness of the *exploration* data set only five cut offs were used for indicator kriging. The cut offs used were those at the 20th, 40th, 60th, 80th and 95th

percentiles (see Figure 3.1.4).

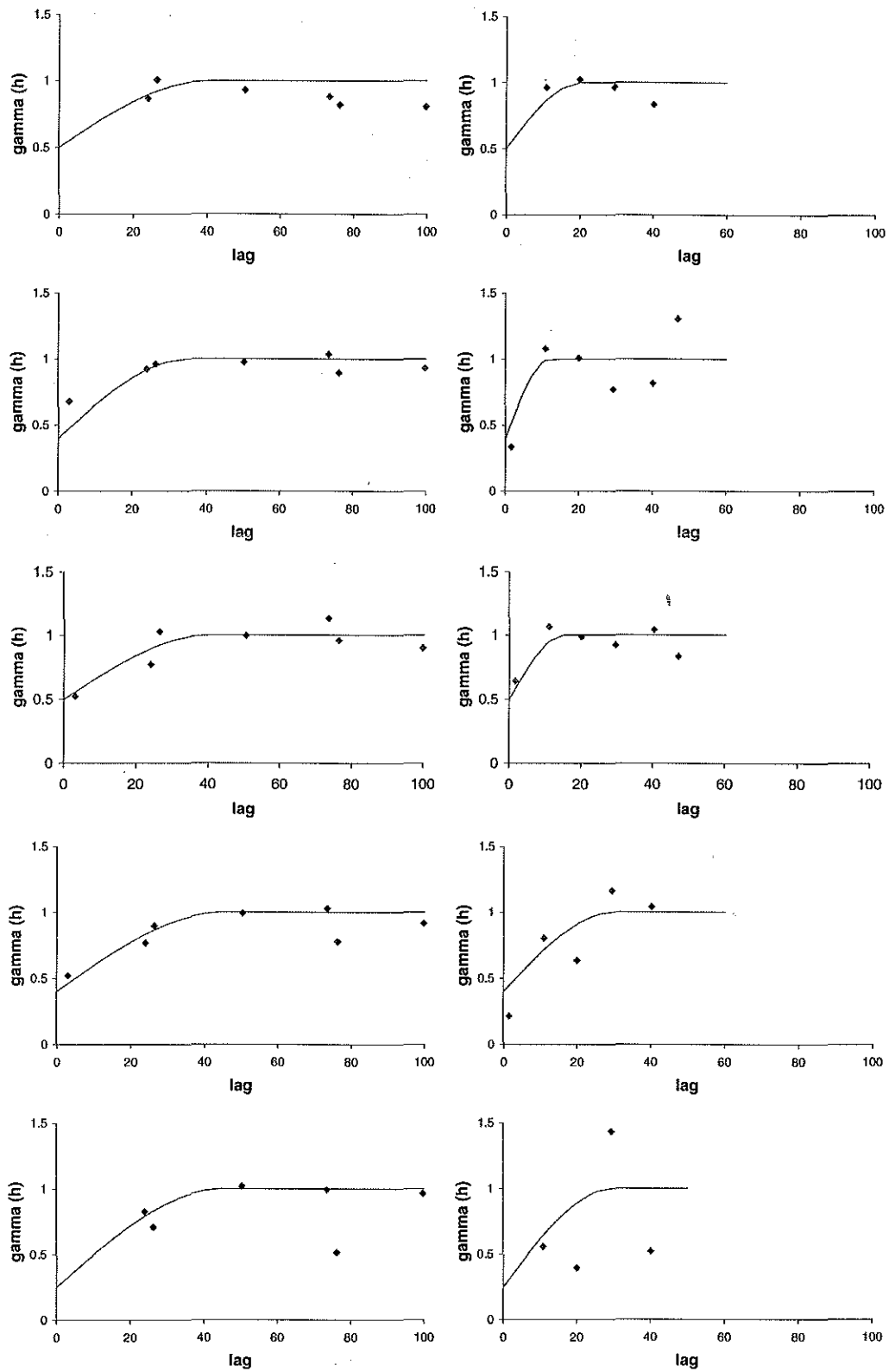


Figure 3.1.4: Experimental and model semivariograms for the *Goodall* data. Cut offs are (top to bottom) 20%, 40%, 60%, 80% and 95%, with N-S on the left and E-W on the right.

Most of the semivariograms have reasonably similar nugget to sill ratios and ranges in the direction of maximum continuity. However the assumption upon which the use of mIK is based, that all semivariograms are proportional, appears to be only approximately satisfied. The semivariogram model at the upper cut off has a relatively low nugget of 0.25. Most other models have nuggets of 0.4 or 0.5, with the exception of the 10th and 50th percentiles. There is much more variation in the ranges in the E-W direction than in the N-S direction, with a minimum range of 10m and a maximum of 35m. In both directions the model for the median cut off has the shortest range.

3.1.3 Results

With such a sparse *exploration* data set several of the bins between the decile cut offs contain no data or only one sample. The number of cut offs used was reduced to six to reduce the number of order relation deviations caused by empty bins. Both mIK and fIK were performed at the 20%, 40%, 60%, 80% and 95% cut offs. The number of samples within each bin is small even with only six cut offs (see Table 3.1.4).

Table 3.1.4. Number of *exploration* data points contained in each bin for the *Goodall* data.

Bin percentiles	Number in bin
[0,20)	2
[20,40)	4
[40,60)	4
[60,80)	6
[80,95)	4
[95,100]	1

The initial estimation for mIK was performed with the model for the 50% semivariogram as the common model. Because of the short range of this model and the sparseness and irregular spacing of the *exploration* data set, for approximately 24% of all locations the distance between the closest *exploration* sample datum and the point to be estimated was greater than the semivariogram range. At these locations all kriging weights were zero and the global cumulative distribution function was reproduced as the estimate. The slightly longer semivariogram range of the 60% semivariogram halved the number of locations at which this occurred. For this reason, and because the model seemed more representative of the other models, the 60% semivariogram was chosen as the common semivariogram model for mIK. Non-estimation was less of a problem with fIK where ranges of the individual semivariograms varied from 35 m to 45 m (see Table 3.1.3).

E-type estimates were calculated from the ccdf obtained by both mIK and fIK and, while there is little difference between the two, neither gives good results when compared with the *blasthole* data (see Figure 3.1.5). Nearly all grade estimates lie between 1.0 and 5.0 g/t and there are no estimates of grades higher than 15.0 g/t. The *blast hole* data contain many grades outside this range. The only region with estimates above 5g/t corresponds to a region of high grades from the *blast hole* data, but all other regions where the true grades are high have low-grade estimates.

Although both methods perform poorly with this data set, fIK produces more estimates of high grades and also more estimates of very low grades than mIK. This is also borne

out by the histograms and summary statistics of the two sets of E-type estimates (see Figure 3.1.6 and Table 3.1.5)

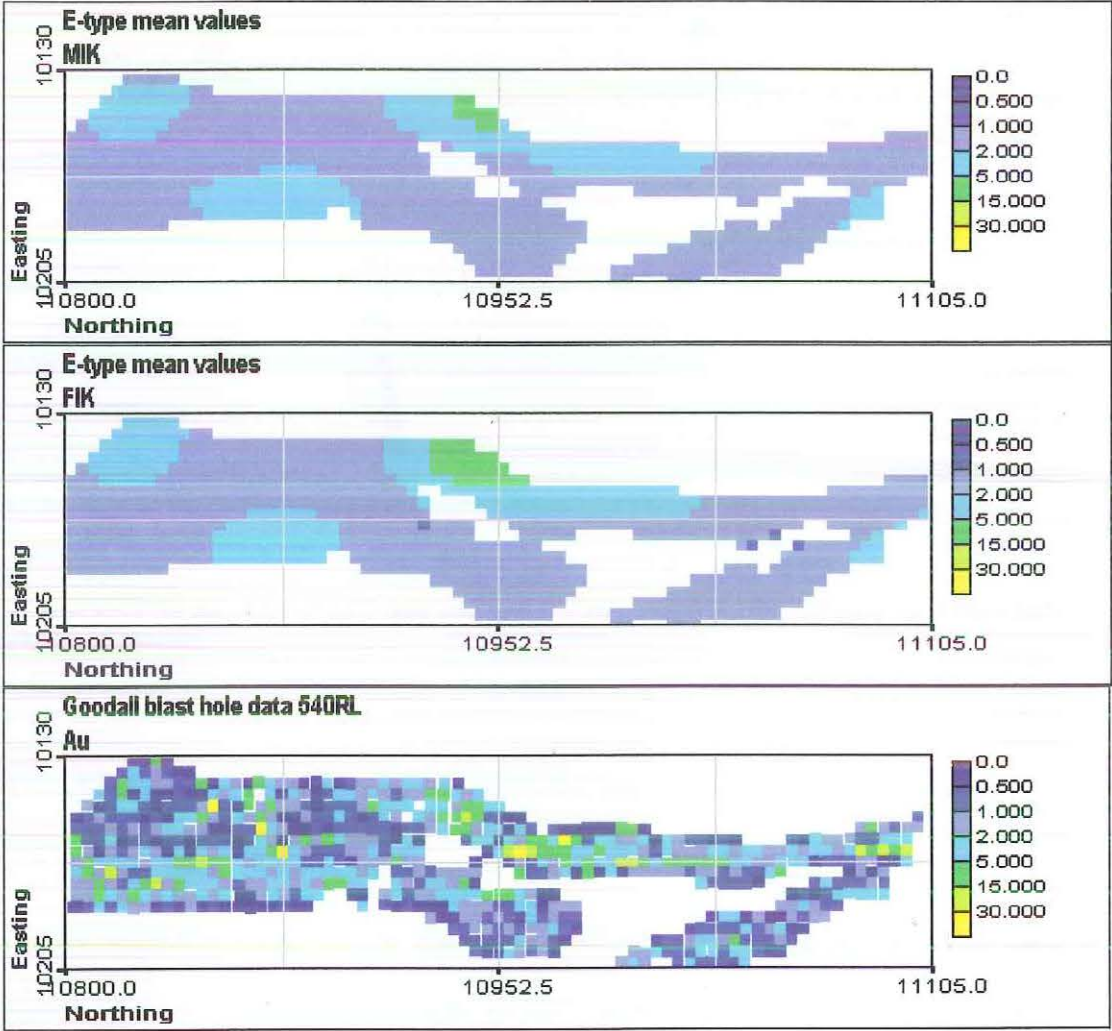


Figure 3.1.5. mIK (top) and fIK (middle) E-type estimates and blast hole data (bottom)

Table 3.1.5. Comparison of summary statistics for the *Goodall* data suite.

Data set	Mean	Median	Standard Deviation	Minimum	Maximum	Skewness
mIK	2.00	1.92	0.60	1.05	7.27	4.46
fIK	2.02	1.76	1.08	0.92	9.62	3.77
Exploration	2.27	1.25	2.92	0.05	12.68	2.57
Blasthole	2.77	1.42	4.62	0.01	49.30	4.80

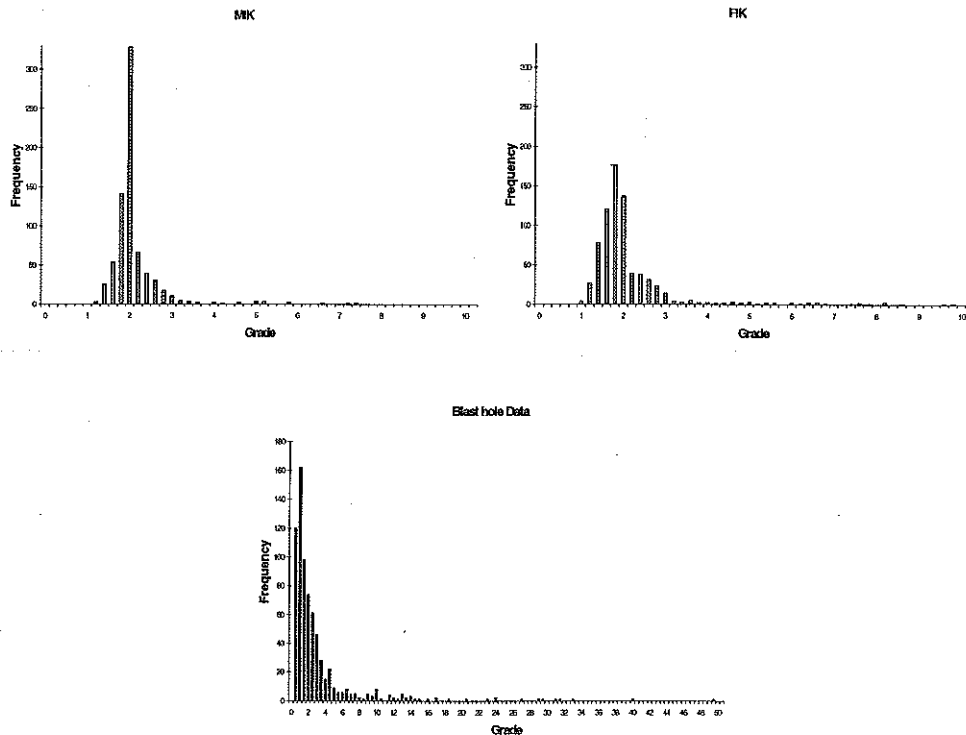


Figure 3.1.6. Histograms of mIK (top left) and fIK (top right) E-type estimates and *blast hole* grades (bottom).

The distributions of both sets of estimates are much more highly skewed than the *exploration* data. This is likely to be due to the fact that the *variography* data set is highly skewed. None of the summary statistics of the *exploration* data have been reproduced very well by either mIK or fIK. In both cases the mean is underestimated, the median is overestimated and the standard deviation is much lower than that of the *exploration* data. The *blast hole* data has a still higher standard deviation.

At this stage the differences between the two methods do not appear to be large enough to warrant the extra time and effort needed to perform fIK. There may be more pronounced differences between the grade tonnage curves for the two methods which could lead to a different decision.

3.1.4 Order Relation Deviations

Very few order relation deviations were encountered, especially considering the small number of *exploration* data. There were none for mIK, and for fIK there were 0.87% with an average magnitude of 0.0113. It was noted that slight changes to the semivariogram model affected both the amount and average magnitude of order relation deviations. For example, removing the nugget from the model at the 95th percentile caused a rise in the number of deviations to 3.06% with an average magnitude of 0.0451.

3.1.5 Grade Tonnage Curves

All data were treated as point data in two-dimensional space rather than block data. The grade tonnage curves were calculated on the assumption that each value of the *blasthole* data and each estimate is representative of a block of size 4m by 4m by 2.5m centred on the location of the datum. No block support correction was applied because point estimates were compared with point support grade control data.

To calculate the average grade above a cut off it was necessary to extrapolate above the highest cut off. As the distribution is highly skewed and a maximum possible value is not known, a hyperbolic extrapolation was used. Several values of ω and ϕ_{\max} were tried, as is shown in Tables 3.1.6 and 3.1.7, and all combinations produced very little difference between the average grades calculated from mIK and fIK estimates. The curves produced cannot simply be compared with that from the exhaustive data to find the closest match, as in actual practice the exhaustive data would not be available. As

the distribution was known to be highly skewed it was decided to use $\omega = 1.5$ to produce a long tail. To reduce the amount of underestimation of the average grade above the highest cut off ϕ_{\max} was set to 0.9975. The grade tonnage curves are given in Figure 3.1.7 and there is very little difference between the two predicted curves.

Table 3.1.6. Average grade above cut off for various values of omega and phimax - mIK.

mIK	Omega	1	1.5	1.5	2
	Phimax	0.995	0.99	0.9975	0.99
cut off	Tonnage	average grade			
0.3	61538	2.50	2.16	2.32	2.11
0.66	46671	3.14	2.70	2.90	2.63
1.23	31910	4.16	3.51	3.81	3.40
2.39	15163	6.76	5.40	6.01	5.16
6.05	3504	15.21	9.31	11.98	8.29

Table 3.1.7. Average grade above cut off for various values of omega and phimax - fIK.

fIK	Omega	1	1.5	1.5	2
	Phimax	0.995	0.99	0.9975	0.99
cut off	Tonnage	average grade			
0.3	61937	2.52	2.18	2.33	2.12
0.66	46450	3.19	2.74	2.95	2.67
1.23	31917	4.22	3.56	3.86	3.45
2.39	15710	6.70	5.37	5.97	5.14
6.05	3533	15.26	9.33	11.99	8.30

Both methods produce tonnage and average grade estimates that are lower than the actual values from the *blast hole* data for all cut offs. Having noted the lack of high grades in the E-type estimates and histograms this is as expected. The differences between the two sets of estimates, which were apparent from the histograms and

summary statistics, appear to have had little or no effect on the grade tonnage curves. A comparison of the average grades shown in Tables 3.1.6 and 3.1.7 shows virtually no difference between the two sets of results. The largest variation is only 0.06g/t and the tonnages are also very similar. These results suggest that with this data set there is no need to use the more time consuming fIK rather than mIK, even though the underlying assumptions for mIK are not completely satisfied.

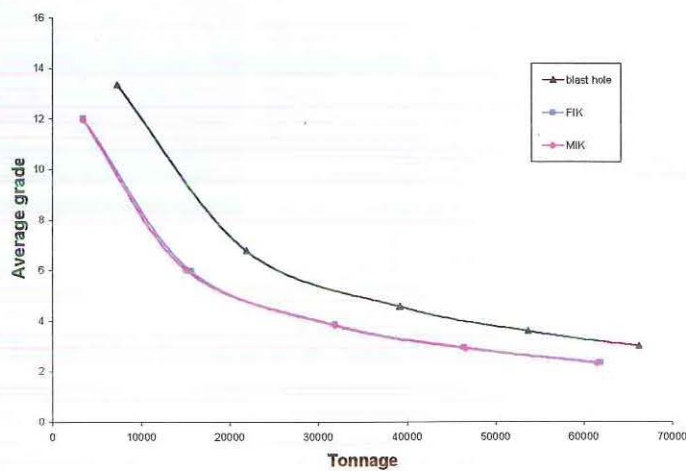


Figure 3.1.7. Grade tonnage curves for mIK and fIK estimates and *blast hole* data.

3.2 True Data Suite

3.2.1 Data Sets

The *True* data are provided with the GSLIB software as an example set. GSLIB provides data for both a primary and a secondary variable but only the primary variable is considered here. The exhaustive set consists of 2500 data values created by simulated annealing to match the first lag of an isotropic semivariogram with a low

nugget (Deutsch and Journel, 1992). The data are located on a two dimensional square grid of size 50 units x 50 units, with a grid spacing of one unit (see Figure 3.2.1). The values obtained by this simulation are typical of those found in gold deposits, allowing the data to be treated as gold mineralisation data.

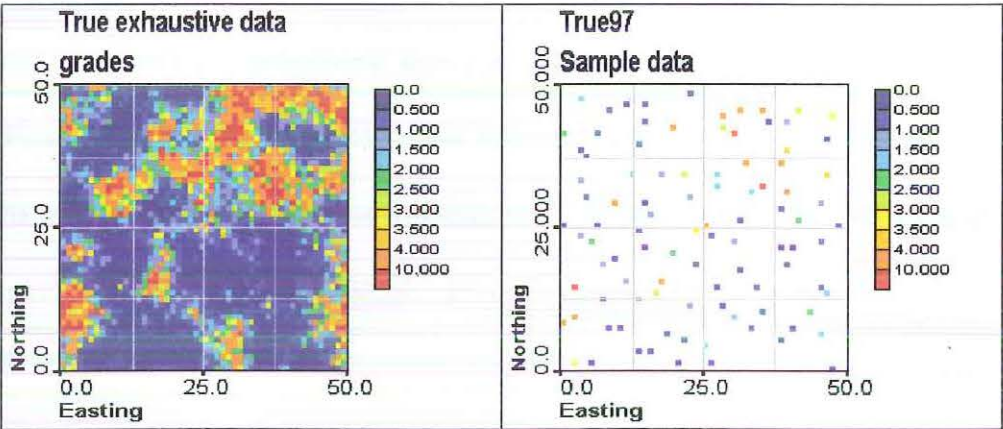


Figure 3.2.1. *True* exhaustive data set (left) and *True97* sample data.

Of the two sets of sample data provided with the GSLIB software, the one used here is a sample of 97 values on a pseudo-regular grid, taken from the exhaustive data set. This sample, which will be called *True97*, was used as the exploration data set for modelling and estimation (see Figure 3.2.1).

Table 3.2.1. Summary statistics for the *True97* and *True* data sets.

Data set	N	Mean	Median	Standard Deviation	Minimum	Maximum	Skewness
<i>True97</i>	97	2.28	1.10	3.22	0.09	18.76	3.03
<i>True</i>	2500	2.58	0.96	5.15	0.01	102.70	6.84

Although this exploration set contains 97 samples it is still relatively sparse. Slightly less than 4% of the exhaustive data are available for variography and estimation.

Summary statistics of the *True97* and *True* data sets are given in Table 3.2.1. The exhaustive data set is more highly skewed and also has a higher standard deviation than the *True97* sample set.

3.2.2 Variography

In order to identify any anisotropy, semivariogram surfaces were drawn for each cut off (see Figure 3.2.2). As they reveal no apparent anisotropy at any cut off isotropic models were fitted to all semivariograms. Experimental semivariograms were calculated at the deciles and the 95th percentile using the parameters given in Table 3.2.2.

Table 3.2.2: Experimental semivariogram parameters.

Lag spacing	2.50
Lag tolerance	1.25
Number of lags	10
Angular tolerance	90°

All semivariograms were fitted with a single spherical structure plus nugget (see Table 3.2.3). Nugget to sill ratios vary from 0 to 1.5 and ranges vary from 2.75 to 12.00, which suggests that the semivariograms are not all proportional to one another (see Figure 3.2.3). There is a reasonable degree of similarity between models above the 40% cut off, with the sole exception of the 95% cut off. Once again the assumptions of mIK are only approximately satisfied.

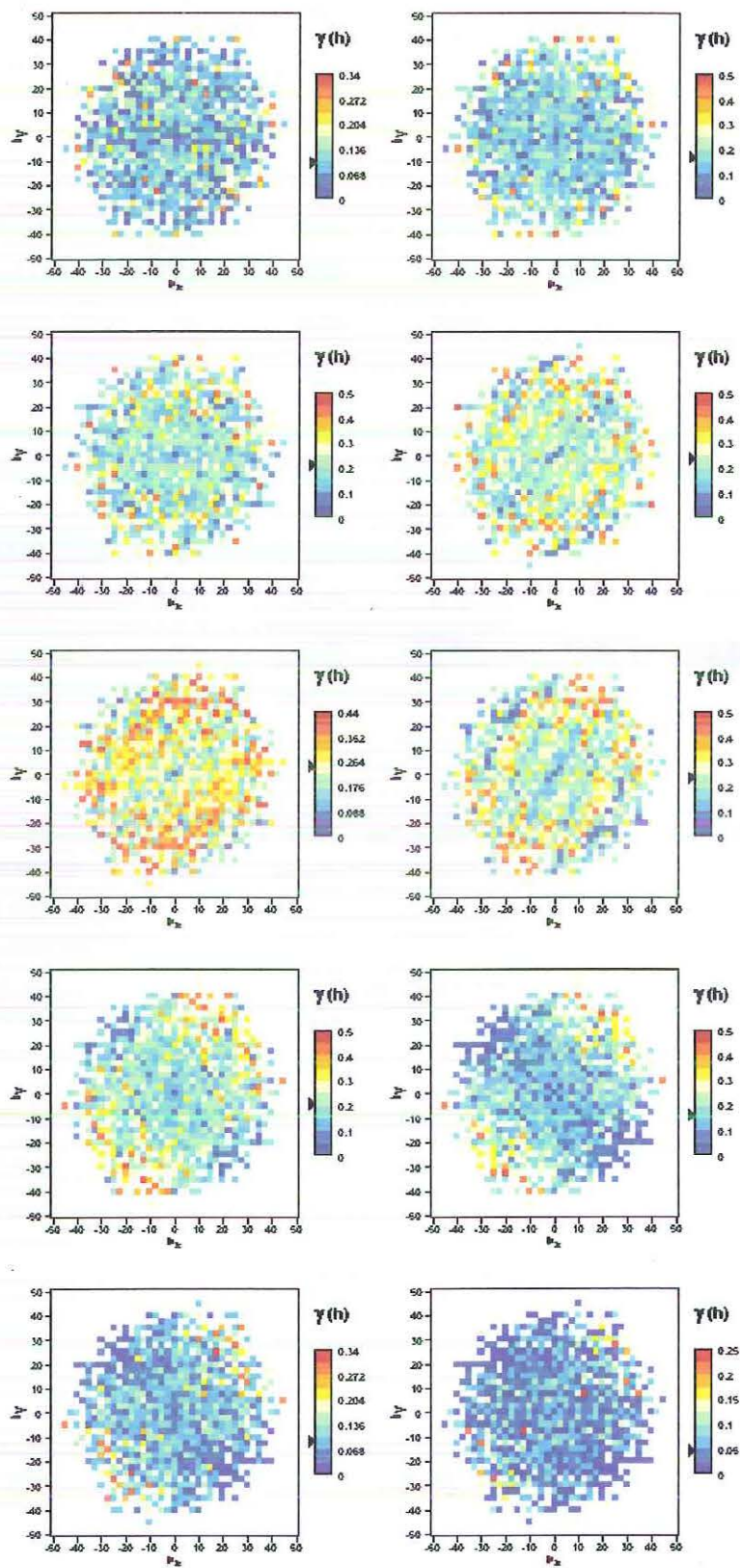


Figure 3.2.2. Semivariogram surfaces for the ten cut offs for the *True97* data set. Cut offs increase reading across and down the page.

Table 3.2.3: *True97* semivariogram models for each of ten cut offs.

cut off		Semivariogram parameters – spherical model plus nugget		
percentage	grade	nugget	partial sill	range
10	0.16	0.20	0.80	7.75
20	0.28	0.10	0.90	7.25
30	0.46	0.00	1.00	6.25
40	0.83	0.20	0.80	6.25
50	1.02	0.40	0.60	9.25
60	1.38	0.45	0.55	9.75
70	2.01	0.35	0.65	10.25
80	3.03	0.40	0.60	12.00
90	5.69	0.50	0.50	10.00
95	8.09	0.60	0.40	2.75

The three sets of cut offs used are given in Table 3.2.4 below. The median semivariogram was used as the common model, except for when only five cut offs were used. In this case the 60% semivariogram was used as the common model. There were only minor differences between the 50% and 60% models so it was expected that this would make little difference to the results.

Table 3.2.4. The three sets of cut offs used for kriging with *True97*.

Number of cut offs	Cut off percentiles
5	20, 40, 60, 80, 95
6	10, 30, 50, 60, 80, 95
10	10, 20, 30, 40, 50, 60, 70, 80, 90, 95

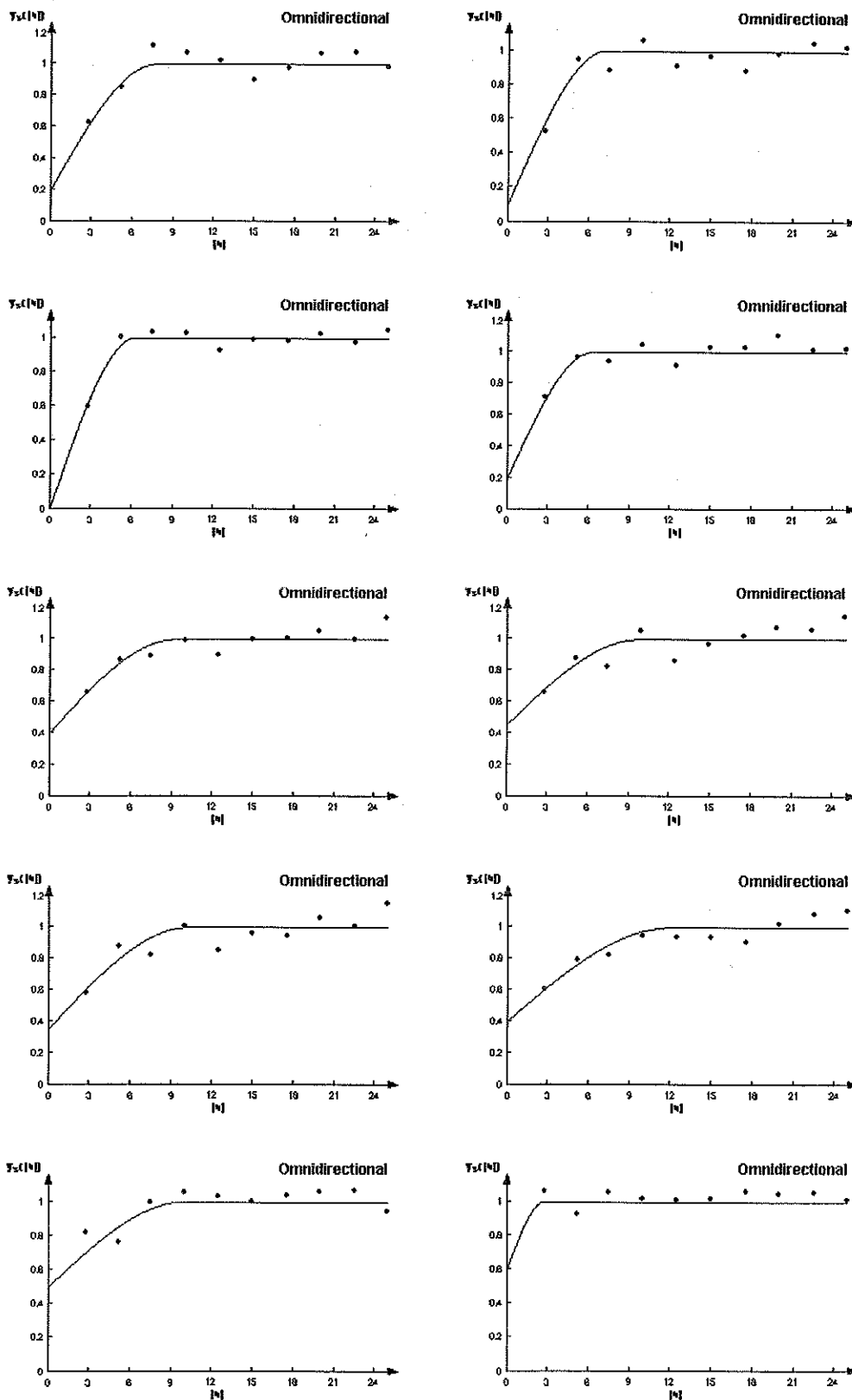


Figure 3.2.3. Semivariogram models for the ten cut offs for *True97*. Cut offs increase reading across and then down the page.

3.2.3 Results

As the *True97* exploration data set contains almost one hundred samples, it was expected that there would be no problems with empty bins when performing the kriging. The numbers of exploration data within each bin are given in Table 3.2.5. Even though there are no empty bins it was decided to perform the kriging using various combinations of cut offs to see what effect, if any, different cut offs had.

Table 3.2.5. Number of exploration data in each bin for the *True* data.

Bin Percentiles	Bin Grades	Number in bin
[0, 10)	[0, 0.16)	11
[10, 20)	[0.16, 0.28)	10
[20, 30)	[0.28, 0.46)	9
[30, 40)	[0.46, 0.83)	9
[40, 50)	[0.83, 1.02)	10
[50, 60)	[1.02, 1.38)	10
[60, 70)	[1.38, 2.01)	9
[70, 80)	[2.01, 3.03)	9
[80, 90)	[3.03, 5.69)	10
[90, 95)	[5.69, 8.09)	5
[95, 100]	[8.09, ∞)	5

E-type estimates were obtained and mosaic maps are shown in Figure 3.2.4. They show little difference between mIK and fIK estimates for each set of cut offs. The choice of cut offs used leads to only minor differences in estimates. A comparison of plots of the E-type estimates with the plot of the exhaustive data set indicates that the estimates are quite good. Although the estimates provide a smoothed map it does not appear to be over-smoothed as were the *Goodall* estimates.

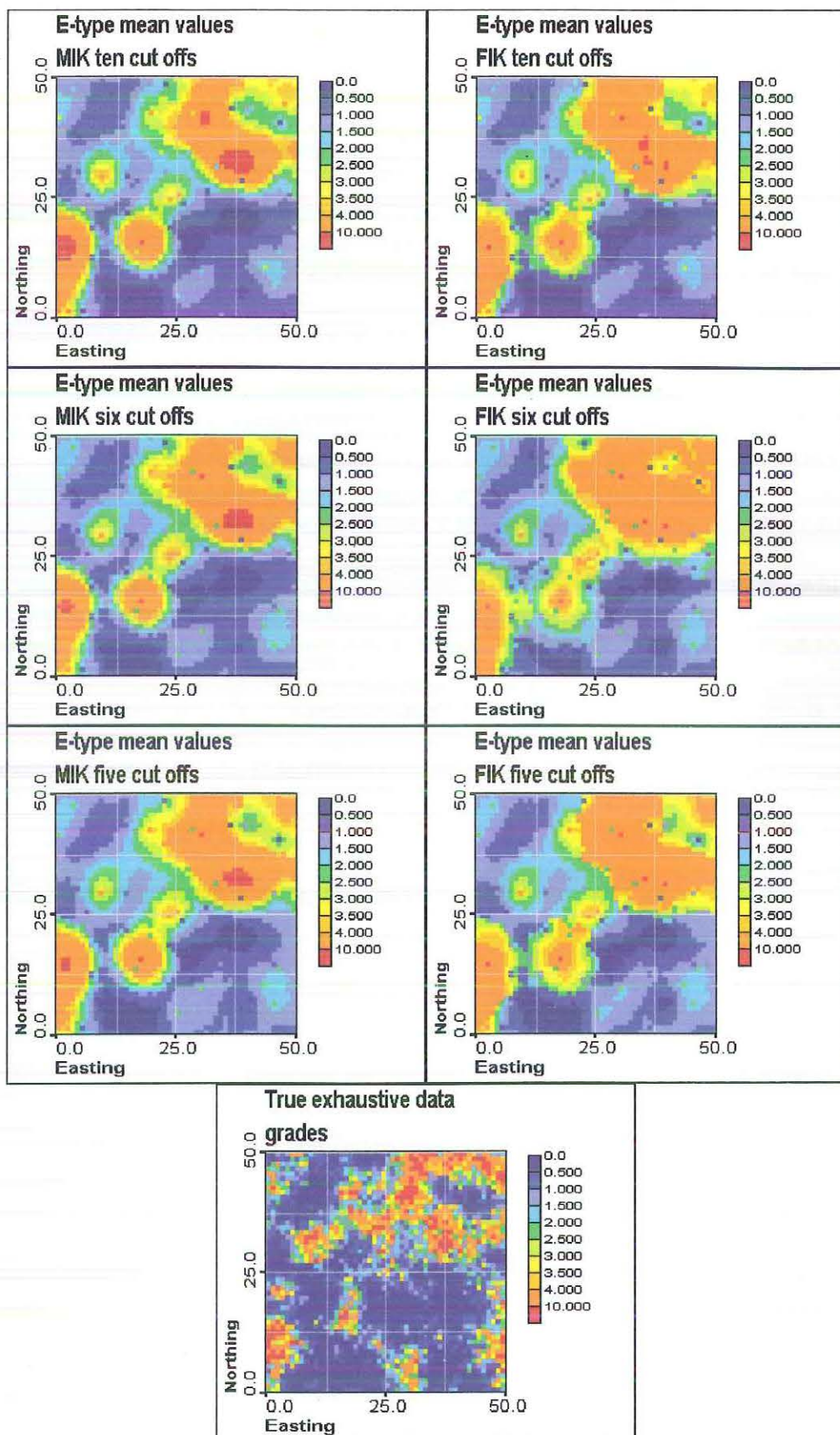


Figure 3.2.4. E-type estimates for various numbers of cut offs. mIK results are on the left and fIK results on the right, with the exhaustive data on the bottom.

The region of high valued estimates in the N-E corner matches a high valued region of the exhaustive data. Within this region the exhaustive data shows a smaller region with low values, which has been overestimated by both methods. With six cut offs fIK overestimates the low values more than mIK and also more than either method with five or ten cut offs. The smaller high-grade regions in the N-W and S-E have been underestimated by each method.

Median IK produces more estimates above ten than fIK, regardless of the number of cut offs used, as can be seen by the small areas of red in the N-E and S-W. The median and 60% semivariogram models have ranges of 9.25 and 9.75 respectively, while the semivariogram for the 95% cut off has a range of only 2.75. The model used for mIK therefore overestimates the spatial continuity at the highest cut off and this is why it produces more high grades than fIK.

Marginally better results were obtained by using ten cut offs, but the different semivariogram model used for five cut offs made no appreciable difference.

Scatterplots of estimates versus the true values (see Figure 3.2.5) show that high values are underestimated by both methods. Although mIK overestimates the spatial continuity at the 95% cut off the grades produced are lower than the actual grades. There are no major differences between any of the scatterplots.

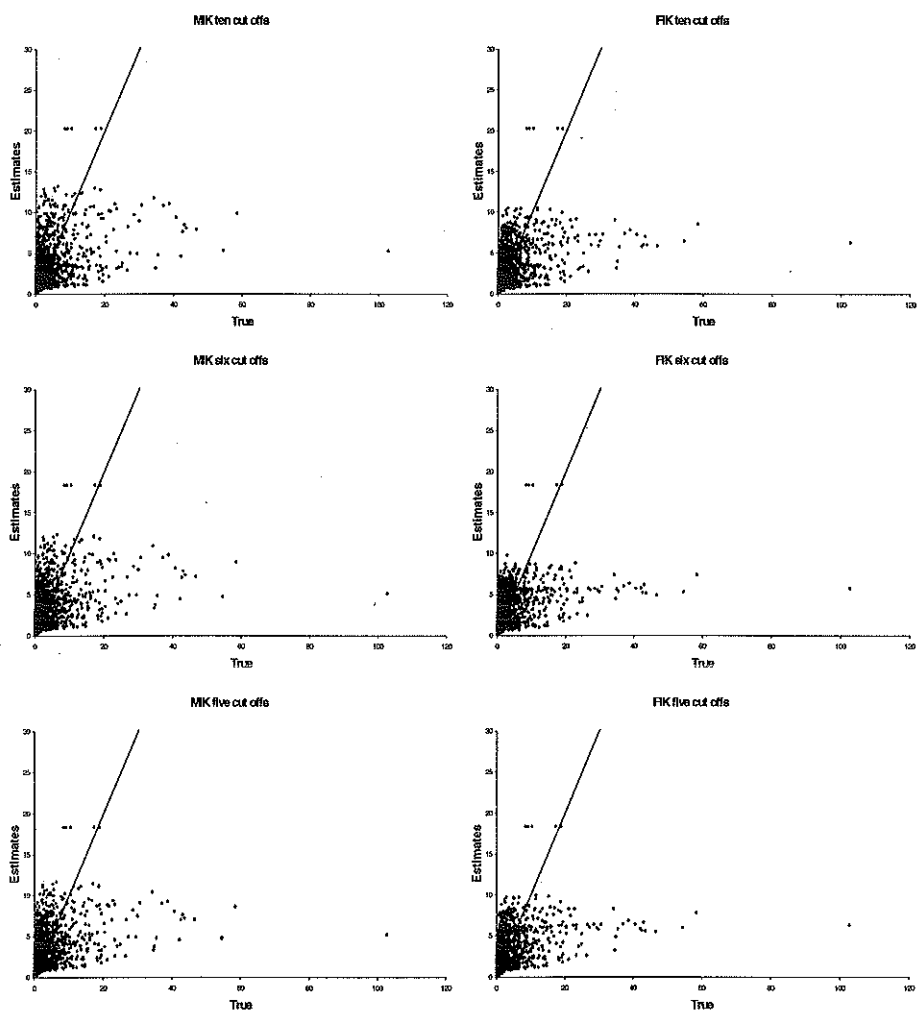


Figure 3.2.5. Scatterplots of E-type estimates versus actual grades for the *True* data. mIK results are shown on the left and fIK results on the right.

Histograms and summary statistics of the estimates and the actual exhaustive data (see Figure 3.2.6 and Table 3.2.6) show that the estimated data are less highly skewed. Although the actual mean is reproduced the estimated distributions all have higher medians and much lower standard deviations than the actual distribution. The means of the estimated distributions are close to the mean of the sample data but the medians are higher than the sample median. The standard deviation and skewness are both underestimated. There is very little difference between any of the histograms or summary statistics of the estimates.

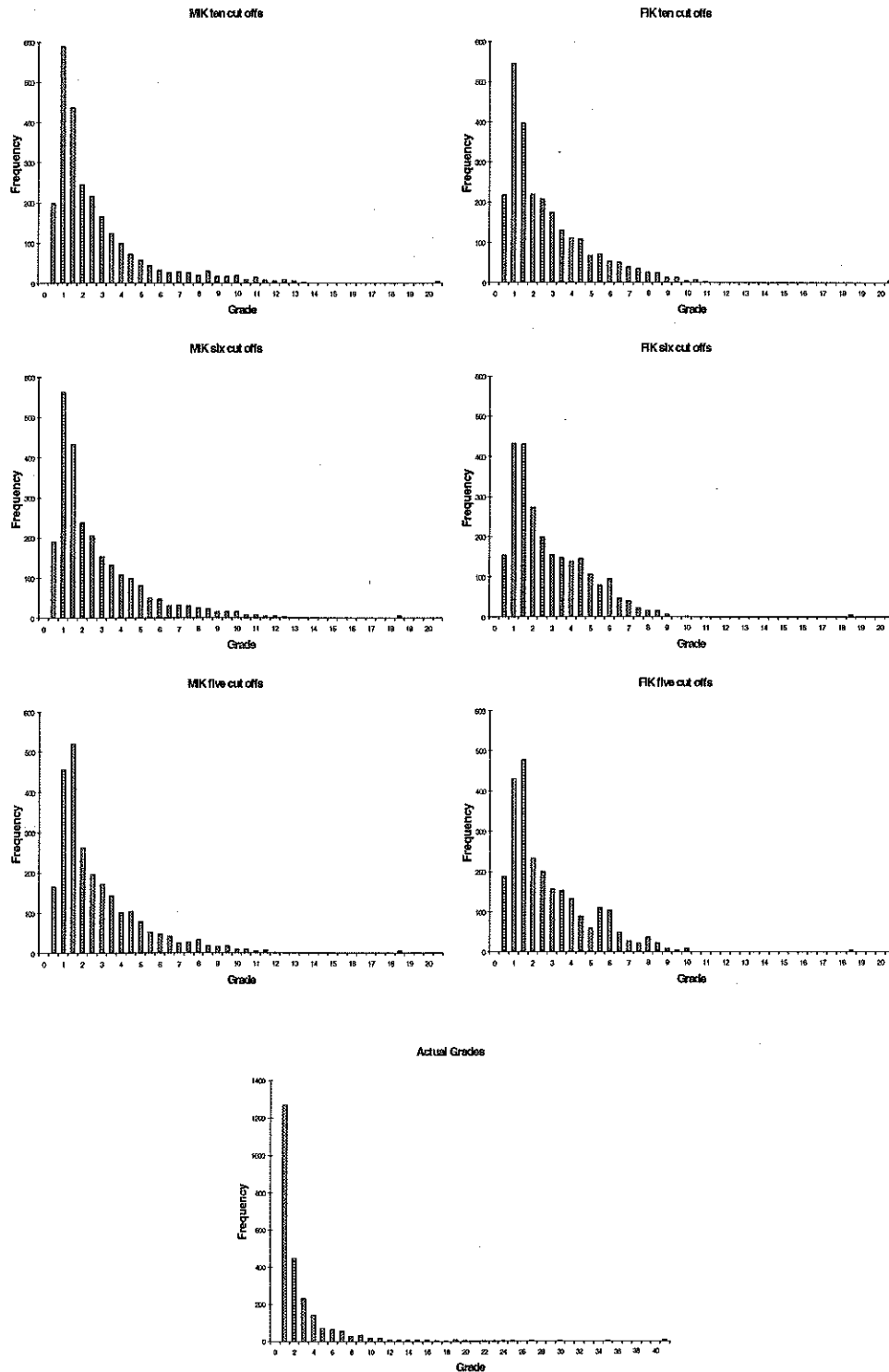


Figure 3.2.6. Histograms of E-type estimates and *True* exhaustive data with mIK on the left and fIK on the right. The horizontal axis of the histogram of the exhaustive data stops at a grade of 40, however the maximum grade is over 100.

Table 3.2.6. Comparison of summary statistics for the *True* data suite.

Data set	Mean	Median	Standard Deviation	Minimum	Maximum	Skewness
mIK (10)	2.48	1.54	2.50	0.08	20.27	2.33
fIK (10)	2.48	1.68	2.23	0.08	20.27	2.07
mIK (6)	2.49	1.61	2.33	0.08	18.33	2.04
fIK (6)	2.57	1.91	2.00	0.08	18.33	1.72
mIK (5)	2.52	1.66	2.24	0.14	18.33	2.02
fIK (5)	2.55	1.79	2.13	0.14	18.33	1.72
<i>True</i> 97	2.28	1.10	3.22	0.09	18.76	3.03
<i>True</i>	2.58	0.96	5.15	0.01	102.70	6.83

3.2.4 Order Relation Deviations

As can be seen from Table 3.2.7, a large number of order relation deviations were encountered with fIK and the combination of cut offs used had a large impact on the amount. Full IK performed best when only five cut offs were used and worst when all ten were used, when corrections were needed for almost 40% of the estimates. Median IK performed much better in this regard, both in the percentage of deviations and the average magnitude of the corrections made.

Table 3.2.7. Order relation deviations for the *True* data.

No. cut offs	Kriging type	%ORD	Av. Mag.
10	fIK	39.50	0.0177
10	mIK	1.62	0.0004
6	fIK	23.14	0.0200
6	mIK	1.64	0.0004
5	fIK	20.14	0.0188
5	mIK	1.81	0.0000

There were slightly more deviations with mIK when the 60% semivariogram model was used, however the average magnitude was zero to four decimal places. The slight change in semivariogram model used for mIK had little effect, however both mIK and fIK were sensitive to larger changes in models. Initial models produced extremely large percentages of order relation deviations for both procedures, over 50% for fIK and 44% for mIK. This emphasises the need for producing a good semivariogram model.

3.2.5 Grade Tonnage Curves

All data were treated as point data in two-dimensional space and no support corrections were made. The point estimates and exhaustive data were assumed to represent blocks centred on the point and of one cubic unit in size. A hyperbolic extrapolation was used to estimate the average grade above the highest cut off.

Tables 3.2.8 to 3.2.13 show the average grades above cut offs for various combinations of ω and ϕ_{\max} . These tables show that there is virtually no difference between the results from mIK and those from fIK regardless of the number of cut offs used. In particular, the average grades determined from mIK are almost identical for the upper cut offs when kriging at five or six cut offs, even though a different semivariogram model was used. There is more difference between the fIK results from these two sets of cut offs but even this variation is small.

Table 3.2.8. Average grade above cut off for various values of omega and phimax – mIK with ten cut offs.

mIK	Omega	1	1.5	1.5	2
	Phimax	0.995	0.99	0.9975	0.99
Cut off	Tonnage	average grade			
0.16	5571	2.80	2.39	2.58	2.32
0.28	4926	3.14	2.67	2.88	2.59
0.46	4373	3.49	2.96	3.20	2.87
0.83	3799	3.92	3.31	3.59	3.21
1.02	3116	4.57	3.84	4.17	3.71
1.38	2472	5.45	4.52	4.95	4.36
2.01	1855	6.70	5.47	6.03	5.25
3.03	1281	8.57	6.79	7.60	6.48
5.69	590	13.50	9.62	11.39	8.96
8.09	292	20.25	12.41	15.98	11.06

Table 3.2.9. Average grade above cut off for various values of omega and phimax – fIK with ten cut offs.

fIK	Omega	i	1.5	1.5	2
	Phimax	0.995	0.99	0.9975	0.99
cut off	Tonnage	Average grade			
0.16	5575	2.80	2.39	2.58	2.32
0.28	4964	3.12	2.66	2.87	2.58
0.46	4416	3.46	2.94	3.18	2.86
0.83	3803	3.92	3.32	3.59	3.21
1.02	3063	4.64	3.89	4.23	3.76
1.38	2459	5.49	4.55	4.98	4.39
2.01	1839	6.77	5.52	6.09	5.30
3.03	1282	8.61	6.82	7.64	6.51
5.69	608	13.33	9.55	11.27	8.90
8.09	293	20.26	12.41	15.98	11.07

Table 3.2.10. Average grade above cut off for various values of omega and phimax – mIK with six cut offs

mIK	Omega	1	1.5	1.5	2
	Phimax	0.995	0.99	0.9975	0.99
cut off	Tonnage	Average grade			
0.16	5571	2.89	2.48	2.67	2.41
0.46	4373	3.60	3.08	3.31	2.99
1.02	3116	4.75	4.02	4.35	3.89
1.38	2472	5.68	4.75	5.17	4.59
3.03	1281	8.91	7.12	7.94	6.82
8.09	292	20.25	12.41	15.98	11.06

Table 3.2.11. Average grade above cut off for various values of omega and phimax – nIK with six cut offs

nIK	Omega	1	1.5	1.5	2
	Phimax	0.995	0.99	0.9975	0.99
cut off	Tonnage	average grade			
0.16	5579	3.02	2.54	2.75	2.46
0.46	4447	3.71	3.11	3.37	3.01
1.02	3100	4.99	4.15	4.51	4.00
1.38	2464	5.97	4.91	5.37	4.72
3.03	1304	9.33	7.31	8.18	6.95
8.09	321	20.87	12.67	16.20	11.22

Table 3.2.12. Average grade above cut off for various values of omega and phimax – mIK with five cut offs

mIK	Omega	1	1.5	1.5	2
	Phimax	0.995	0.99	0.9975	0.99
Cut off	Tonnage	average grade			
0.28	4923	3.28	2.81	3.02	2.73
0.83	3794	4.09	3.48	3.76	3.38
1.38	2471	5.69	4.76	5.18	4.60
3.03	1280	8.92	7.13	7.94	6.82
8.09	293	20.27	12.42	15.99	11.07

Table 3.2.13. Average grade above cut off for various values of omega and phimax – fIK with five cut offs

fIK	Omega	1	1.5	1.5	2
	Phimax	0.995	0.99	0.9975	0.99
Cut off	Tonnage	average grade			
0.28	4950	3.32	2.82	3.04	2.74
0.83	3796	4.15	3.51	3.80	3.40
1.38	2453	5.82	4.83	5.27	4.66
3.03	1286	9.11	7.21	8.05	6.88
8.09	305	20.53	12.53	16.08	11.14

As the distribution is highly skewed it was decided to use $\omega = 1.5$ and $\phi_{\max} = 0.9975$. The grade tonnage curves for all sets of cut offs are shown in Figure 3.2.7. The curves are almost identical in each case, with fIK producing slightly higher average grades than mIK when six cut offs were used. In all cases the predicted curves are only slightly lower than the actual curve for low cut offs. At higher cut offs the difference between actual and predicted curves is more pronounced, although still not large.

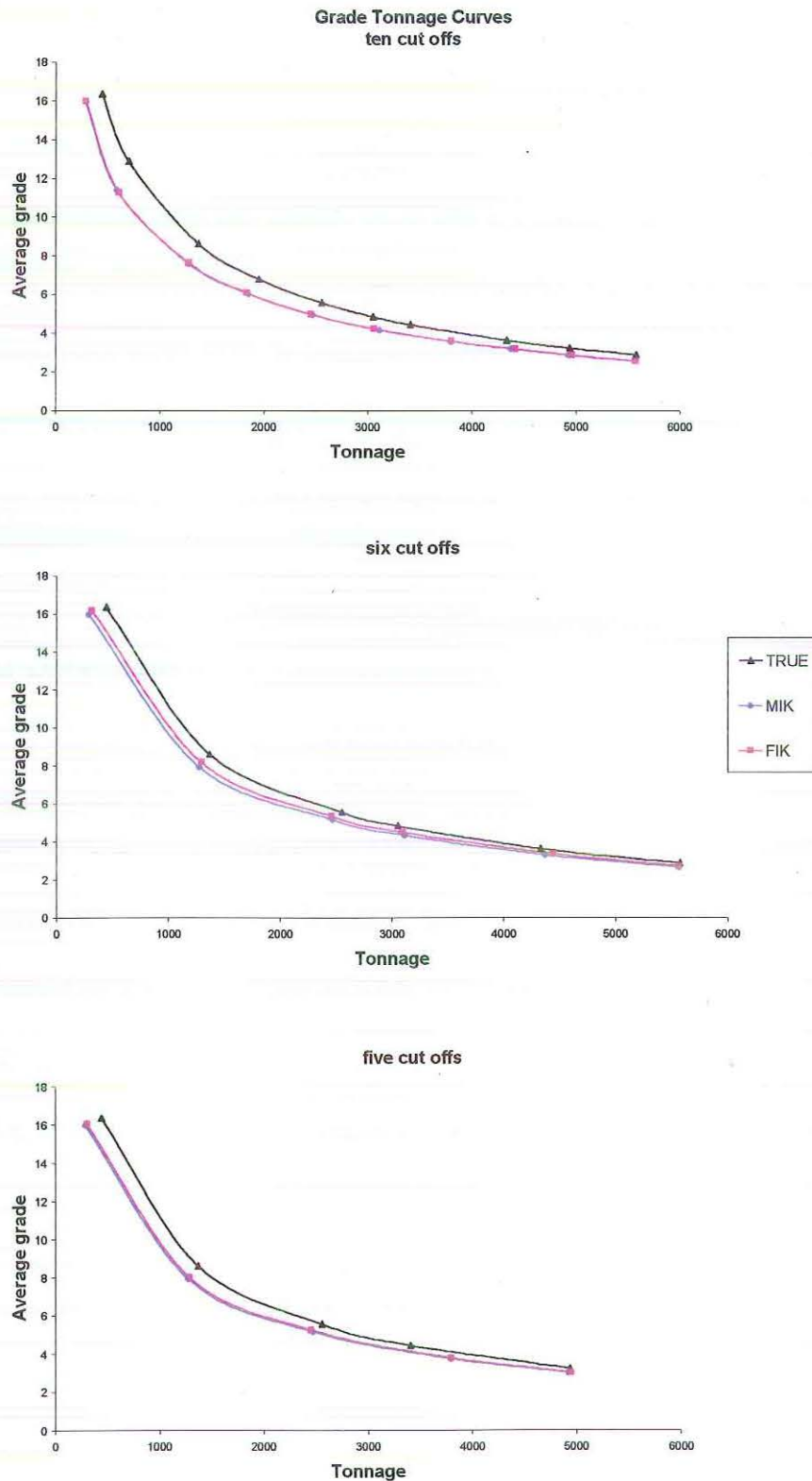


Figure 3.2.7. Grade tonnage curves for mIK and fIK estimates and the exhaustive *True* data set.

It appears from the plots of E-type estimates (Figure 3.2.4) that mIK should produce grade tonnage curves with higher average grades than fIK at the higher cut offs. However, although mIK produces more estimates above a grade of ten, fIK produces fewer estimates below two and slightly more above a grade of five. The plots of E-type estimates, the scatterplots and the histograms are useful in comparing the two methods but from a mining perspective it is more important to be able to accurately estimate recoverable reserves and so the grade tonnage curve is a better tool for comparison. All comparisons show little overall difference between mIK and fIK for this suite of data.

3.3 Berea Data Suite

3.3.1 Data Sets

The exhaustive *Berea* data set contains 1600 air permeability measurements taken from a two-dimensional slab of Berea sandstone (Journel & Alabert, 1989). The exhaustive data are located on a square of size 40 units by 40 units, with a grid spacing of one unit by one unit (see Figure 3.3.1). We created an exploration data set, used for variography and kriging, by taking a random sample of 128 points from the exhaustive data (see Figure 3.3.1). This set will be called *Berea128*. Summary statistics for the two data sets are given below in Table 3.3.1 and are similar, with both data sets approximately normally distributed.

Table 3.3.1. Summary statistics for the two *Berea* data sets.

Data set	N	Mean	Median	Standard Deviation	Minimum	Maximum	Skewness
<i>Berea128</i>	128	55.58	55.00	16.72	24.00	98.00	0.32
<i>Berea</i>	1600	55.53	55.00	15.79	19.50	111.50	0.38

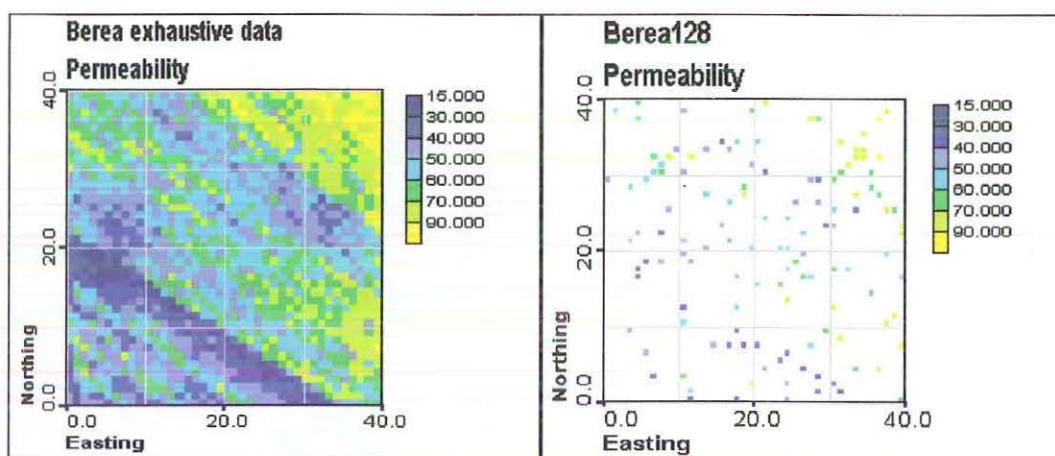


Figure 3.3.1. *Berea* exhaustive data set (left) and *Berea128* sample data.

3.3.2 Variography

Semivariogram surfaces were drawn for the deciles and the 95th percentile to identify any anisotropy. At most cut offs there is evidence of anisotropy (see Figure 3.3.2). The direction of maximum continuity is at a bearing of approximately 125° from N for most cut offs, although it varies slightly between cut offs. At the lowest cut off it is very difficult to identify the direction of maximum continuity. As anisotropy is often more readily apparent from correlograms than from semivariograms (Isaaks & Srivastava, 1989), the correlogram surface for this cut off was also studied (see Figure 3.3.3). The correlogram surface quite clearly shows a single direction of maximum continuity at a bearing of approximately 125°.

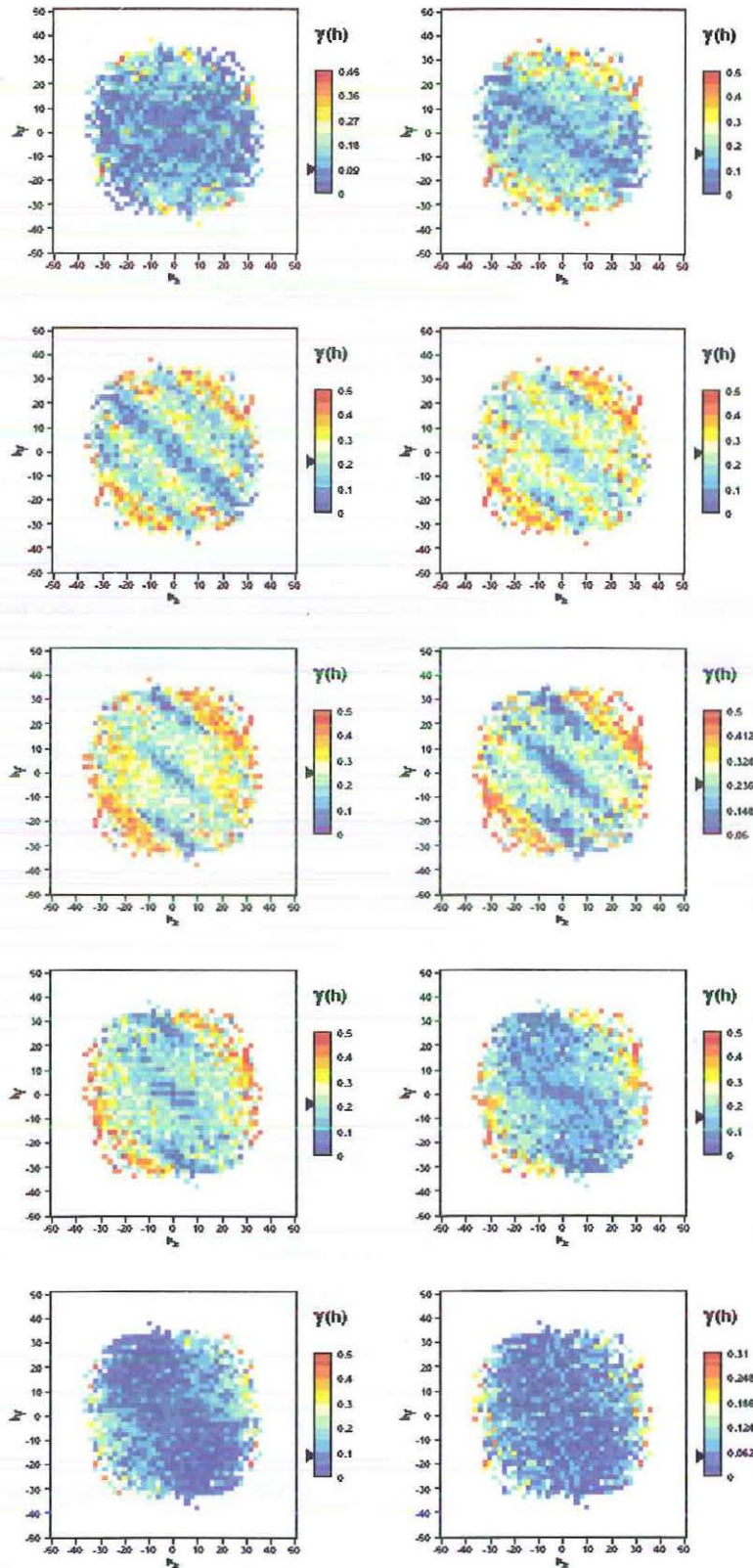


Figure 3.3.2. Semivariogram surfaces for the ten cut offs for the *Boreal28* data. Cut offs increase reading across and then down the page. There is some rotation of the direction of anisotropy. The two highest cut offs do not display anisotropy.

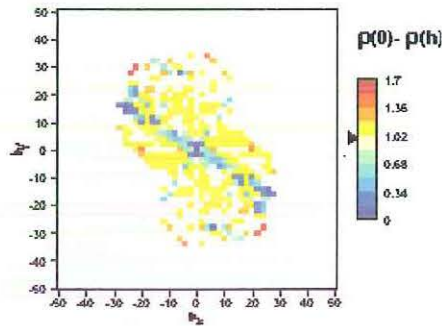


Figure 3.3.3. Correlogram surface for the 10% cut off for *Bereal28*.

For the highest cut offs there is little variation with direction and isotropic models were fitted to the 90% and 95% cut offs. Correlogram surfaces were produced for these cut offs, but were not useful as very few values could be computed. Table 3.3.2 gives the parameters used to calculate experimental semivariograms, while Table 3.3.3 shows the directions of maximum and minimum continuity for each cut off, except the two uppermost.

Table 3.3.2: Experimental semivariogram parameters.

Lag spacing	2
Lag tolerance	1
Number of lags	10
Angular tolerance	22.5°

The change in the direction of anisotropy between cut offs is in most cases only 5°, however between the 70% and 80% cut offs there is a shift of 10°. Large shifts of anisotropy can cause severe order relation problems when using fIK (Deutsch & Journel, 1992) but in this case the angular change is less than the angular tolerance used, so there should be little change in the experimental semivariogram.

Table 3.3.3. Directions of maximum and minimum continuity for *Berea128* data set – all directions given as bearings from N.

	Cut off		Maximum continuity	Minimum continuity
	percentage	permeability		
	10	34.55	305°	35°
	20	40.00	305°	35°
	30	46.05	310°	40°
	40	50.00	310°	40°
	50	55.00	310°	40°
	60	58.60	310°	40°
	70	64.45	315°	45°
	80	70.00	325°	55°

The change from an anisotropic model at the 80% cut off to an isotropic model at the 90% cut off is likely to have a large effect on the number of order relation deviations. Attempts were made to fit anisotropic models to the two highest cut offs to reduce this effect. The directional standardised semivariograms were quite erratic (see Figure 3.3.4) and values could be obtained only for the first four lags in the direction of minimum continuity, which made choosing a model very difficult. The number of order relation deviations was slightly higher at each cut off when the anisotropic models were used. It was therefore decided that there was no benefit in using anisotropic models for the two highest cut offs and the isotropic models were used.

The semivariograms in the direction of maximum continuity reached a lower sill than those in the direction of minimum continuity so zonal anisotropic models were fitted. The model for each cut off consisted of two spherical structures plus nugget, except for the 90% and 95% cut off which were fitted with a single spherical structure plus nugget (see Table 3.3.4, Figures 3.3.5 and 3.3.6). It is apparent that not all are proportional to

each other, with large variations in nugget, sill and range between cut offs.

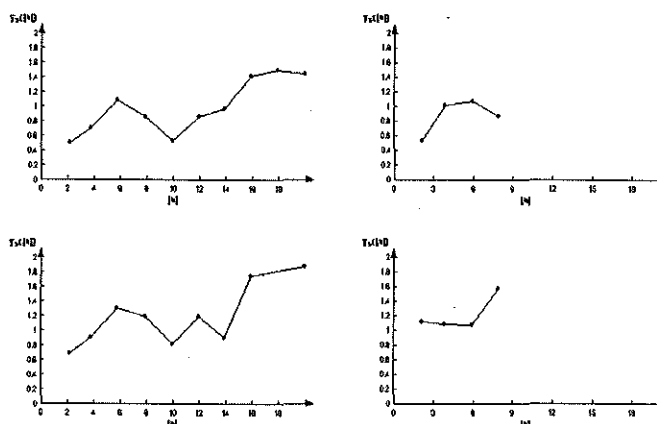


Figure 3.3.4. Experimental semivariograms for 90% (top) and 95% (bottom) cut offs for *Berea128*. The bearings are 325° (left) and 55° (right).

Table 3.3.4. Semivariogram models for the *Berea* data suite. All cut offs except 90% and 95% were fitted with two spherical structures plus nugget.

Cut off	Nugget	Structure number	Partial sill	Range	Anisotropy factor	Bearing
10%	0.00	1	1.00	14.80	1	305°
		2	0.8	18.60	1000	35°
20%	0.00	1	1.00	20.00	1	305°
		2	0.60	5.80	1000	35°
30%	0.10	1	0.70	13.60	1	310°
		2	0.59	7.80	1000	40°
40%	0.40	1	0.44	12.80	1	310°
		2	0.37	8.20	1000	40°
50%	0.27	1	0.52	11.60	1	310°
		2	0.39	6.20	1000	40°
60%	0.20	1	0.68	18.80	1	310°
		2	0.51	7.40	1000	40°
70%	0.41	1	0.55	21.00	1	315°
		2	0.44	3.80	1000	45°
80%	0.33	1	0.60	12.96	1	325°
		2	0.71	12.31	1000	55°
90%	0.39	1	0.61	13.40	1	
95%	0.80	1	0.20	12.00	1	

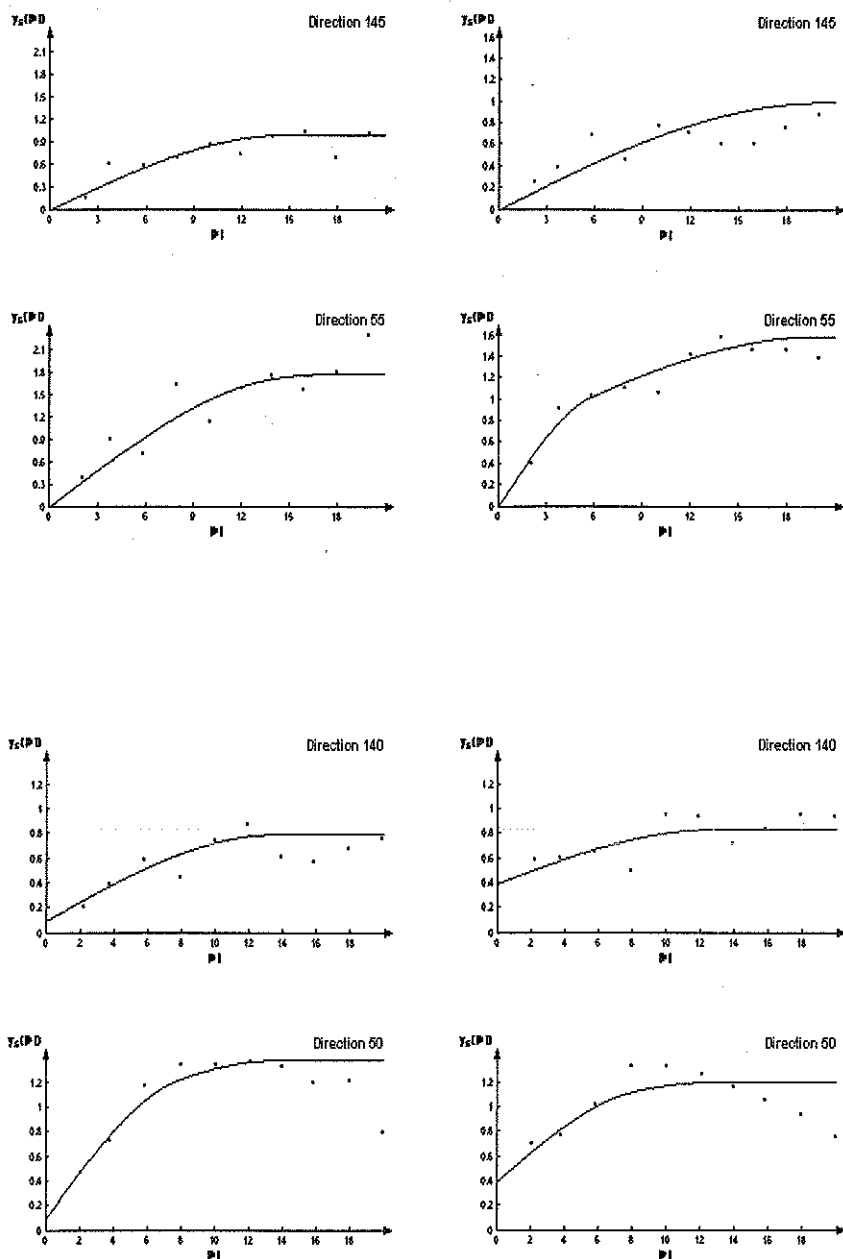


Figure 3.3.5. Semivariogram models for *Boreal28* for the 10% (top left), 20% (top right), 30% (bottom left) and 40% (bottom right) cut offs. The directions of maximum and minimum continuity are shown for each cut off.

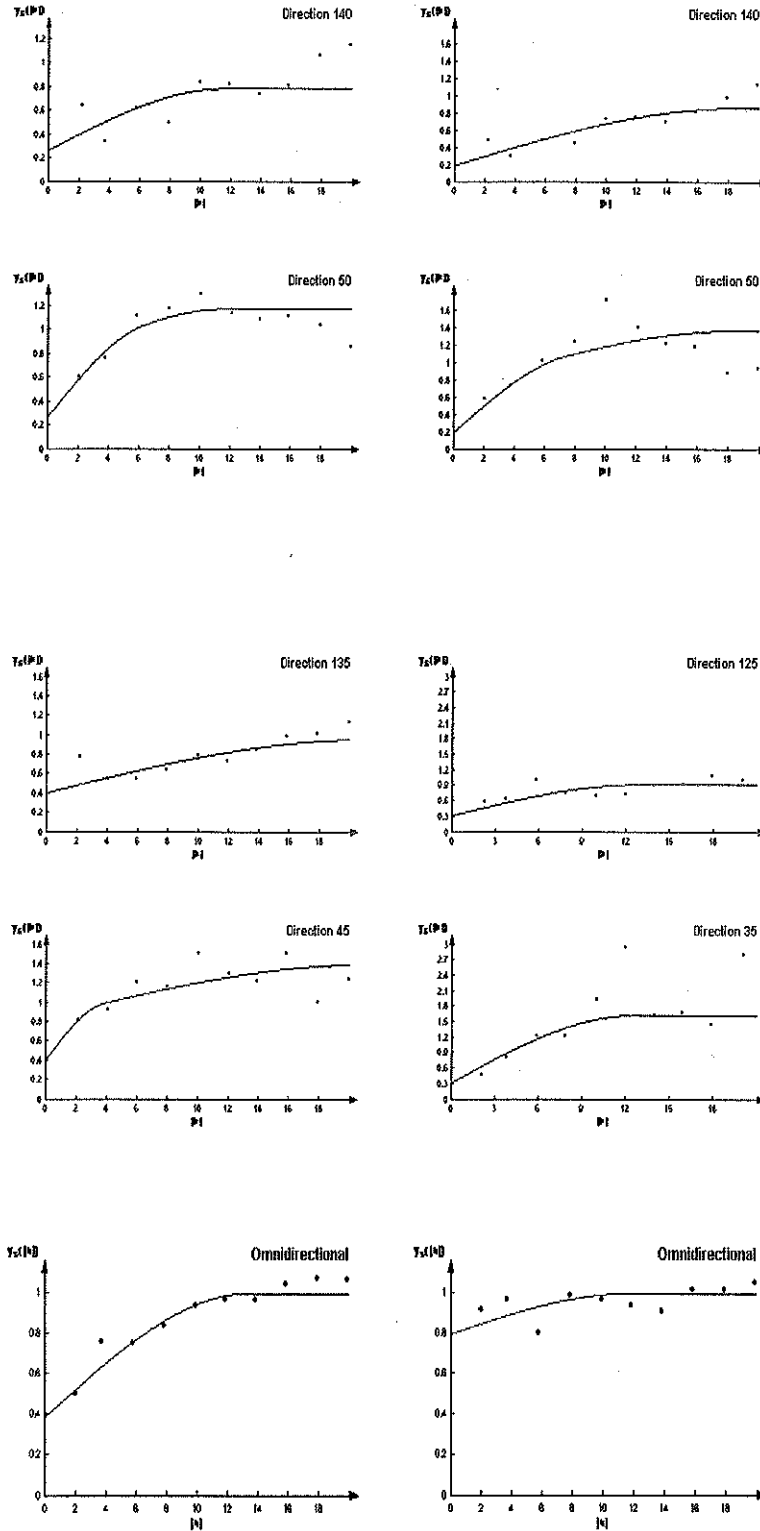


Figure 3.3.6. Semivariogram models for *Berea128* for the 50% (top left), 60% (top right), 70% (centre left), 80% (centre right), 90% (bottom left) and 95% (bottom right) cut offs. The directions of maximum and minimum continuity are shown for each cut off except the 90% and 95% cut offs.

3.3.3 Results

Three sets of cut offs were used for indicator kriging (see Table 3.3.5). The median semivariogram model was used as the common model for mIK in each case. Plots of the E-type estimates calculated from both mIK and fIK ccdf estimates are shown in Figure 3.3.7. Regardless of the method or number of cut offs used, the results appear to be very good.

Table 3.3.5. The three sets of cut offs used for kriging with *Berea128*.

Number of cut offs	Cut off percentiles
5	30, 50, 70, 90, 95
6	10, 30, 50, 70, 90, 95
10	10, 20, 30, 40, 50, 60, 70, 80, 90, 95

The anisotropy apparent from the exhaustive data is reproduced well by both mIK and fIK for all sets of cut offs used. Median IK produces more estimates of high values in the N-E and S-E corners than fIK irrespective of the number of cut offs used, which is surprising as the range of the median semivariogram is less than the ranges of the semivariograms for the three highest cut offs. A comparison with the exhaustive data indicates that mIK may overestimate the number of high values in these regions.

Estimates for the S-W region are consistently lower than the exhaustive data, especially when only five cut offs were used. Differences between the estimates using different numbers of cut offs are minor, with five cut offs providing slightly larger regions with low values. Overall these plots show very little difference between any of the sets of estimates.

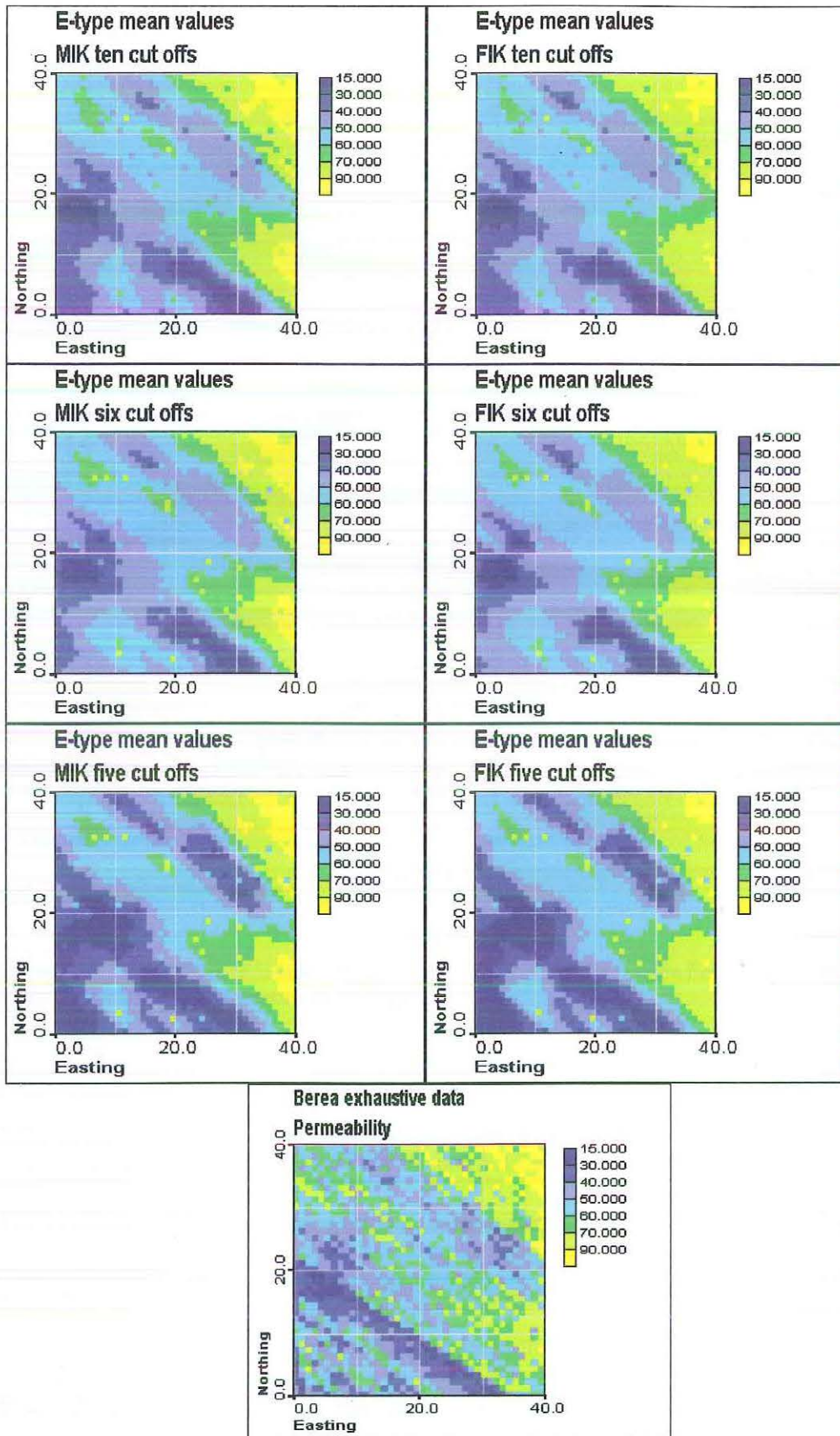


Figure 3.3.7. E-type estimates for mIK (left) and fIK (right), with the exhaustive *Berea* data on the bottom.

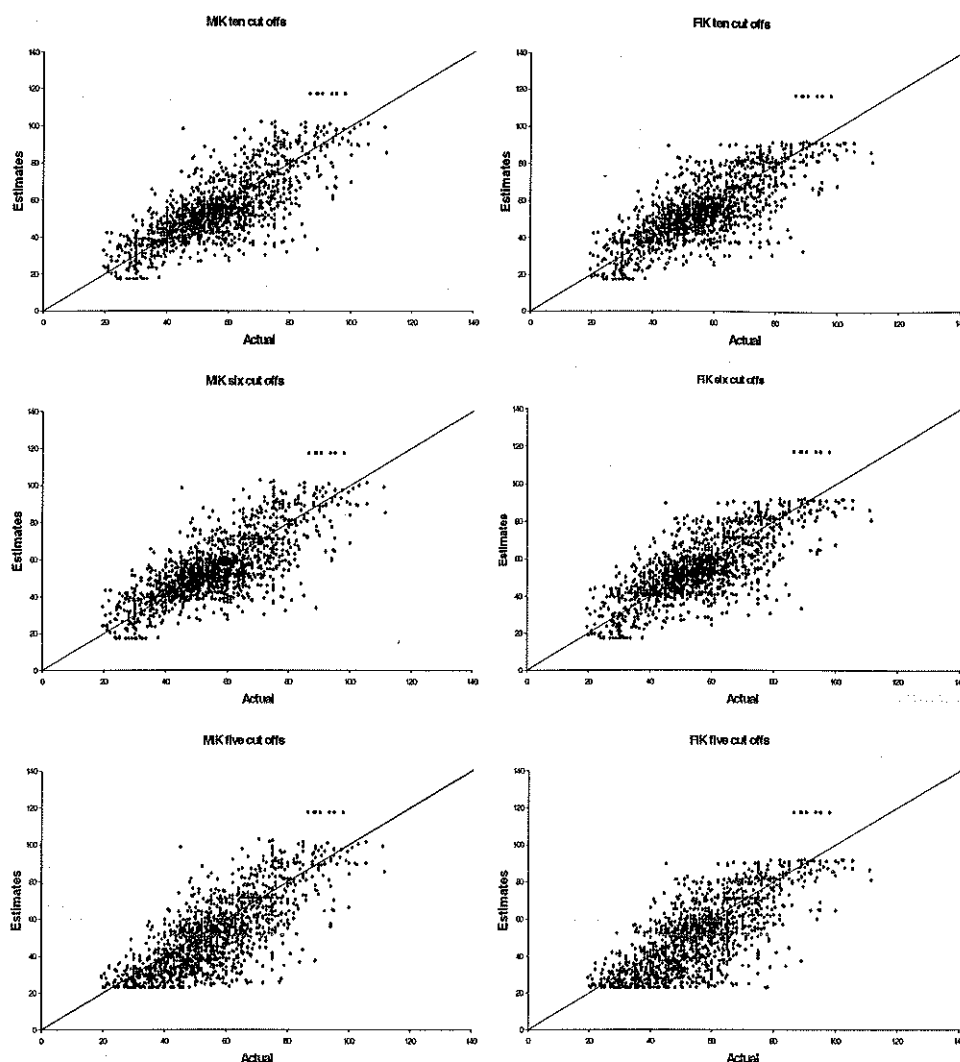


Figure 3.3.8. Scatterplots of E-type estimates versus actual grades for the *Berea* data, with mIK results on the left and fIK results on the right.

Scatter plots of the estimated values versus the actual values show little difference between the different estimations (see Figure 3.3.8). There is also little underestimation of high values or overestimation of low values, which is in contrast to the results from the *True* data set. This is probably due to the approximately normal nature of the actual distribution. When only five cut offs were used there is slightly more underestimation of actual values, but this is the only noticeable difference between any of the scatterplots.

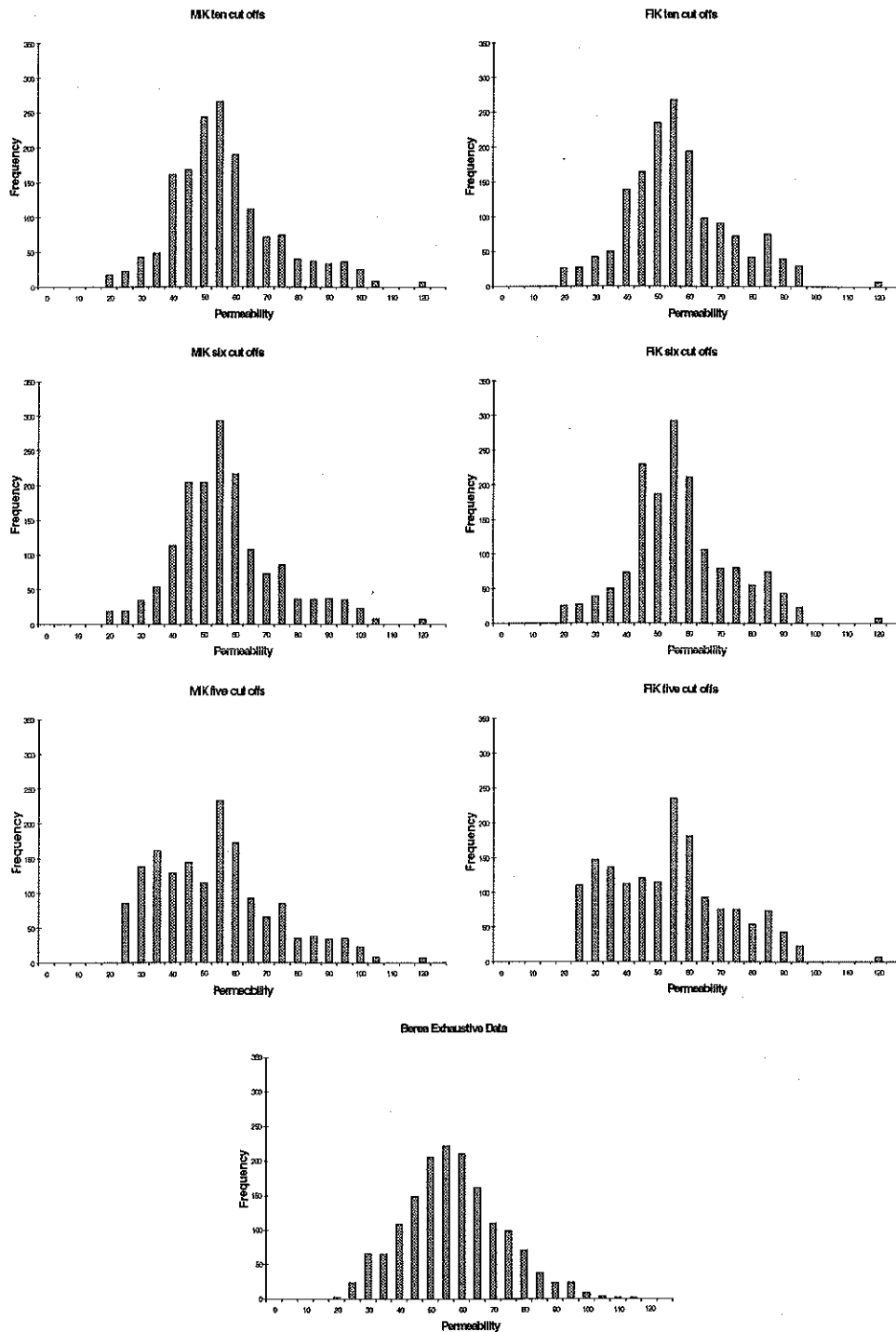


Figure 3.3.9. Histograms of estimated data and exhaustive *Berea* data. mK estimates are shown on the left and fK estimates on the right.

Histograms of the various estimates and exhaustive data (see Figure 3.3.9) show little difference between the two indicator kriging methods but a rather large difference based on the cut offs used. The histogram of estimates obtained from using only five cut offs

shows a large number of low valued estimates, whereas the estimates from using six or ten cut offs have a distribution much more like the actual data.

Table 3.3.6. Comparison of summary statistics for the *Berea* data suite.

Data set	Mean	Median	Standard Deviation	Minimum	Maximum	Skewness
mIK (10)	54.16	51.80	16.91	17.28	117.49	0.79
fIK (10)	54.03	52.27	16.45	17.28	117.49	0.51
mIK (6)	54.71	52.42	16.60	17.28	117.49	0.75
fIK (6)	54.57	52.65	16.20	17.28	117.49	0.46
mIK (5)	51.13	50.52	18.99	23.02	117.49	0.68
fIK (5)	51.06	50.94	18.63	23.02	117.49	0.45
<i>Berea</i> 128	55.58	55.00	16.72	24.00	98.00	0.32
<i>Berea</i>	55.53	55.00	15.79	19.50	111.50	0.38

The summary statistics of the estimated distributions (see Table 3.3.6) show very little difference between the results from using ten or six cut offs. The sample mean and standard deviation have been reproduced in each case, while the median has been only slightly underestimated. The results from using only five cut offs underestimate the sample mean slightly and overestimate the standard deviation. The estimated distributions are in all cases more skewed than the sample and the exhaustive data set, with fIK producing distributions with higher skewness than those produced by mIK.

Overall there is little apparent difference between mIK and fIK, even though in this case the semivariogram models at the upper cut offs were isotropic while the model used for mIK was anisotropic.

3.3.4 Order Relation Deviations

Large numbers of order relation deviations were encountered for both mIK and fIK (see Table 3.3.7). Because the same kriging weights are used at each cut off for mIK there should be very few corrections needed. In this case there were a large number of estimates greater than one or less than zero. Full IK produced more order relation deviations than mIK and with ten cut offs the amount was over 40%. This was almost halved by using fewer cut offs. The number of corrections needed does not appear to have affected the quality of the estimates, as is illustrated by the various comparisons with the actual data (see Figures 3.3.7 to 3.3.9)

Table 3.3.7. Order relation deviations for the Berea data.

No. cut offs	Kriging type	%ORD	Av. Mag.
10	fIK	41.81	0.0251
10	mIK	20.38	0.0115
6	fIK	25.07	0.0200
6	mIK	14.93	0.0107
5	fIK	23.65	0.0162
5	mIK	15.84	0.0107

4. DISCUSSION AND CONCLUSIONS

Median and full indicator kriging results were compared for three suites of data. Each suite contained sample data to be used as conditioning data and exhaustive data which represented reality. The distributions of the two suites representing gold mineralisation data were highly skewed, while the distribution of the third suite was approximately normal. The assumption that all semivariograms were proportional was, at best, only approximately satisfied in each case.

Kriging was performed using different sets of cut offs for the *True* and *Berea* data suites, but only one set was used for the *Goodall* data due to the sparseness of the *exploration* data. Comparisons were made between the results from the different sets of cut offs as well as between those from mIK and fIK.

The results were analysed in several ways. E-type estimates and histograms of the estimates were obtained in each case and compared with the exhaustive data. Scatterplots comparing estimated values with actual values at corresponding locations were drawn for two of the data suites. No scatterplots were drawn for the *Goodall* data suite as the exhaustive data were not located exactly on a grid and so the estimates and actual data were not co-located. Predicted grade tonnage curves were drawn for the two suites representing gold grades and compared with the actual curves.

4.1 Discussion

The sparseness of the *exploration* data set from the *Goodall* data suite led to a high number of locations having no nearby sample data. If the distance to the nearest sample datum was larger than the range of the semivariogram model being used all kriging weights became zero and the value of the global cdf was reproduced as the estimate. This occurred more often with mIK because the same semivariogram model and hence the same kriging weights were used at each cut off.

A different semivariogram model was used for each cut off with fIK and so the ranges varied. Although the kriging weights were all zero for some locations at some cut offs, there were fewer locations at which they were zero for all cut offs. The model for the 60% semivariogram had a longer range than that of the median and so was used as the common model for mIK to try to overcome this problem. The *True* and *Berea* data suites were less sparse and this problem was not encountered with these data suites.

Comparisons of plots of E-type estimates and actual data indicated that both mIK and fIK provided good estimates for the *True* and *Berea* data suites, but not for the *Goodall* data suite. In all cases these plots showed only minimal differences between the two methods. There were also very few differences between the different sets of cut offs used for the *True* and *Berea* data. This was even though a different common semivariogram model was used with one set of cut offs for the *True* data suite. With the *Berea* data the disparities between results from different sets of cut offs were more pronounced than those between mIK and fIK.

Very little difference could be seen between the various scatterplots for the *True* or the *Berea* data suites. The *Berea* estimates appeared to be very good, with little underestimation of high values or overestimation of low values. The scatterplots clearly showed that the estimates from the *True* data were less highly skewed than the actual data. This was also seen from the histograms, which are very similar irrespective of the method or the number of cut offs used. The histograms of the *Berea* estimates are similar when ten or six cut offs are used, but there is a difference when only five are used. The number of low values has been substantially overestimated in this case.

The grade tonnage curves calculated for mIK and fIK were very similar. The only instance in which there was a slight difference between the two results was when kriging with six cut offs for the *True* data suite. The other grade tonnage curves were almost indistinguishable. The curves for the *Goodall* data underestimated the actual curve, especially at the higher cut offs. The curves for the *True* data only slightly underestimated the actual curve. Tables of the average grades above cut offs showed that in nearly every case the only difference between the two methods was in the second decimal place.

4.1.1 Order Relation Deviations

Very few order relation deviations were encountered for the *Goodall* data suite. Less than one percent of estimates needed correcting for fIK and the average correction was approximately 0.01, while there were no corrections needed with mIK. This may have been partially due to the locations at which the global cdf was reproduced as an estimate

and partially due to the reasonably smooth changes in semivariogram models between cut offs.

When using mIK with the *True* data suite the number of order relation deviations encountered was minimal, however there were a large number with fIK. Slightly less than two percent of mIK estimates needed correction but over twenty percent of fIK estimates had to be corrected. When all ten cut offs were used the number of corrections needed for fIK was almost forty percent. The average magnitude of the corrections was much less for mIK than for fIK. Both mIK and fIK were extremely sensitive to changes in the semivariogram models in regard to the number of order relation deviations.

Both mIK and fIK produced a large number of order relation deviations with the *Berea* data suite. When performing mIK few order relation problems are usually encountered because the same kriging weights are used for each cut off. In this instance there were many estimates outside the interval $[0, 1]$ which were all corrected by setting the estimate to the nearest bound of the interval. With mIK the number of order relation deviations varied from approximately fifteen percent, when five or six cut offs were used, to twenty percent when ten cut offs were used. The number encountered when using fIK varied from twenty three percent to over forty percent.

There was little difference between mIK and fIK estimates for any data suite and the number of cut offs used also had little effect on the estimates. The only major differences were with the number of order relation deviations, where mIK performed better than fIK, as expected.

4.2 Conclusions

This thesis has shown comparisons of median indicator kriging and full indicator kriging with three different data suites. The data distributions varied from very highly skewed to approximately normal and the exploration data sets showed various degrees of sparseness. In each case there were only minor differences between the output of the two methods and using mIK reduced the number of order relation deviations. Using different sets of cut offs produced very little difference between estimates, but sometimes large differences in order relation deviations.

Median IK is used rather than fIK to save time and effort, however checking that the assumptions for using mIK are satisfied is nearly as time consuming as performing fIK. In practice this check is therefore often omitted. The results from these three data suites with differing distributions indicate that mIK performs equally as well as fIK in all three cases, even though the assumptions of mIK are, at best, only approximately satisfied. However, this may not be a general result and one should not simply use mIK without at least a cursory check on the validity of the assumptions.

It is also important to choose the common semivariogram model carefully, particularly when the sample data set is sparse. The extra time and effort taken to model several semivariograms at cut offs close to the median, rather than simply choosing the median cut off, can produce better results.

Finally, the results obtained from the *Goodall* data were poor. This may have been due to the combination of the sparseness and highly skewed nature of the *exploration* data set, rather than either one of these factors alone. Even though both mIK and fIK

produced similar results it appears that neither method is satisfactory with this particular data set. In fact better results have been obtained from this data set using sequential Gaussian fractal simulation (Kentwell, Bloom & Comber, 1997).

REFERENCES

- Buxton, B. E., Wells, D. E., & Diluise, G. (1997). Comparison of three kriging methods for making soil remediation decisions. In E. Y. Baafi & N. A. Schofield (eds.), *Geostatistics Wollongong '96, Volume 2* (pp.984-995). Dordrecht: Kluwer Academic Publishers.
- Carr, J. R., & Bailey, R. E. (1986). An indicator kriging model for investigation of seismic hazard. *Mathematical Geology*, 18 (4), 409-428.
- Clark, I. (1979). *Practical geostatistics*. London: Applied Science Publishers Ltd.
- Cressie, N. A. C. (1991). *Statistics for spatial data*. New York: John Wiley & Sons
- David, M. (1988). *Handbook of applied advanced geostatistical ore reservation estimation*. Amsterdam: Elsevier.
- Davis, J. C. (1986). *Statistics and data analysis in geology. Second edition*. New York: John Wiley & Sons.
- Deutsch, C. V., & Journel, A. G. (1992). *GSLIB: Geostatistical software library and user's guide*. New York: Oxford University Press.
- Deutsch, C. V., & Journel, A. G. (1998). *GSLIB: Geostatistical software library and user's guide 2nd edition*. New York: Oxford University Press.
- Fytas, K., Chaouai, N.-E., & Lavigne, M. (1990). Gold deposits estimation using indicator kriging. *CIM Bulletin*, 83 (934), 77-83.
- Glacken, I., & Blackney, P. (1998). A practitioners implementation of indicator kriging. In J. Vann (ed.), *Proceedings of a one day symposium: Beyond Ordinary Kriging*. Perth: Geostatistical Association of Australasia.
- Goovaerts, P. (1994). Comparison of coIK, IK and mIK performances for modeling conditional probabilities of categorical variables. In R. Dimitrakopoulos (ed.), *Geostatistics for the next century* (pp.18-29). Dordrecht: Kluwer Academic Publishers.
- Goovaerts, P. (1997). *Geostatistics for natural resources evaluation*. New York: Oxford University Press.
- Guarascio, M., David, M., & Huijbregts, C. (eds.). (1976). *Advanced geostatistics in the mining industry*. Dordrecht: D. Reidel Publishing Company.
- Hill, D. L., Mueller, U. A., & Bloom, L. M. (1998). Comparison of median and full indicator kriging in the analysis of a gold mineralisation. In J. Vann (ed.), *Proceedings of a one day symposium: Beyond Ordinary Kriging*. Perth: Geostatistical Association of Australasia.

- Isaaks, E. H., & Srivastava, R. M. (1989). *An introduction to applied geostatistics*. New York: Oxford University Press.
- Journal, A. G. (1983). Nonparametric estimation of spatial distributions. *Journal of the International Association for Mathematical Geology*, 15 (5), 445-468.
- Journal, A. G. (1988). Nonparametric geostatistics for risk and additional sampling assessment. In L. H. Keith (ed.), *Principles of environmental sampling* (pp45-72). USA: American Chemical Society.
- Journal, A. G., & Alabert, F. (1989). Non-Gaussian data expansion in the earth sciences. *Terra Nova*, 1 (2), 123-134.
- Journal, A. G., & Huijbregts, C. J. (1978). *Mining geostatistics*. London: Academic Press.
- Kanevski, M., Savelieva, E., Chernov, S., Demyanov, V., & Timonin, V. *3Plot program for Windows 95*. May 1998.
- Kentwell, D. J. (1997). *Fractal relationships and spatial distributions in ore body modelling*. Unpublished masters thesis, Edith Cowan University, Perth, Western Australia.
- Kentwell, D. J., Bloom, L. M., & Comber, G. A. (1997). Improvements in grade tonnage curve prediction via sequential Gaussian fractal simulation. *Mathematical Geology* (to appear).
- Pan, G., & Arik, A. (1993). Restricted kriging for mixture of grade models. *Mathematical Geology*, 25 (6), 713-736.
- Pannatier, Y. (1996). *Variowin: Software for spatial data analysis in 2D*. New York: Springer-Verlag
- Quick, D. (1994). Geology of the Goodall gold mine. *Proceedings of the AUSIMM annual conference, Darwin August 1994*. 75-82.
- Smith, J. L., Halvorson, J. J., & Papendick, R. (1993). Using multiple variable indicator kriging for evaluating soil quality. *Soil Science Society of America Journal*, 57 (3), 743-749.
- Vann, J., & Guibal, D. (1998). Beyond ordinary kriging – an overview of non-linear estimation. In J. Vann (ed.), *Proceedings of a one day symposium: Beyond Ordinary Kriging*. Perth: Geostatistical Association of Australasia.
- Wackernagel, H. (1995). *Multivariate geostatistics*. Berlin: Springer.

APPENDIX A – Sample Data Sets

Goodall exploration set

Exploration composites 540RL

5

Northing

Easting

Elevation

Au

zero

10898.96	10154.20	538.75	1.06	0
11000.07	10178.87	538.74	0.05	0
10947.87	10171.24	538.75	1.08	0
10948.43	10144.03	538.75	12.68	0
11049.63	10175.81	538.75	0.54	0
10846.27	10160.30	538.75	0.31	0
11102.01	10181.02	538.75	5.52	0
11047.54	10178.34	538.76	0.23	0
10996.27	10157.20	538.75	4.99	0
10800.00	10152.24	538.75	0.76	0
10825.00	10146.38	538.75	5.26	0
10825.00	10174.72	538.75	1.93	0
10849.90	10148.60	538.75	0.38	0
10849.60	10162.85	538.75	1.25	0
10876.50	10143.17	538.75	1.65	0
10875.00	10174.95	538.75	3.97	0
10900.10	10139.15	538.75	1.54	0
10900.10	10168.95	538.75	1.5	0
10925.00	10168.81	538.75	0.53	0
10950.00	10173.54	538.75	1.42	0
11075.00	10161.97	538.75	1.11	0

True97 data set

True97 conditioning data

3

Xlocation

Ylocation

Primary

39.5	18.5	0.06	3.5	33.5	1.1
5.5	1.5	0.06	11.5	15.5	1.11
38.5	5.5	0.08	22.5	30.5	1.21
20.5	1.5	0.09	45.5	29.5	1.21
27.5	14.5	0.09	13.5	12.5	1.27
40.5	21.5	0.1	22.5	11.5	1.34
15.5	3.5	0.1	17.5	34.5	1.36
6.5	25.5	0.11	39.5	43.5	1.37
38.5	21.5	0.11	3.5	23.5	1.38
23.5	18.5	0.16	30.5	22.5	1.38
0.5	25.5	0.16	46.5	13.5	1.66
9.5	19.5	0.17	30.5	9.5	1.7
36.5	43.5	0.18	27.5	32.5	1.71
21.5	5.5	0.19	12.5	34.5	1.78
13.5	3.5	0.19	25.5	4.5	1.81
40.5	7.5	0.19	27.5	34.5	1.82
31.5	17.5	0.22	45.5	6.5	1.89
46.5	40.5	0.24	3.5	47.5	1.96
10.5	7.5	0.26	33.5	31.5	1.98
28.5	11.5	0.28	41.5	26.5	2.13
8.5	7.5	0.28	19.5	20.5	2.17
47.5	0.5	0.31	0.5	41.5	2.33
4.5	37.5	0.32	5.5	22.5	2.34
14.5	21.5	0.33	43.5	10.5	2.47
22.5	48.5	0.34	41.5	45.5	2.75
18.5	6.5	0.34	28.5	42.5	2.76
3.5	38.5	0.34	21.5	34.5	2.84
11.5	46.5	0.4	16.5	13.5	2.99
31.5	26.5	0.45	23.5	24.5	3.04
14.5	29.5	0.46	2.5	1.5	3.33
14.5	43.5	0.51	47.5	44.5	3.35
38.5	28.5	0.57	39.5	38.5	3.51
45.5	14.5	0.62	46.5	34.5	3.81
4.5	30.5	0.65	35.5	45.5	4.6
6.5	41.5	0.67	25.5	25.5	4.89
7.5	12.5	0.71	28.5	44.5	5.05
26.5	23.5	0.79	19.5	42.5	5.15
8.5	45.5	0.81	38.5	36.5	5.31
14.5	46.5	0.83	2.5	9.5	6.26
13.5	24.5	0.84	32.5	36.5	6.41
26.5	1.5	0.89	0.5	8.5	6.49
33.5	7.5	0.92	31.5	45.5	7.53
45.5	22.5	0.93	9.5	29.5	8.03
48.5	25.5	0.94	39.5	31.5	8.34
35.5	10.5	0.96	17.5	15.5	9.08
34.5	14.5	0.99	2.5	14.5	10.27
13.5	39.5	0.99	30.5	41.5	17.19
7.5	18.5	1.01	35.5	32.5	18.76
15.5	27.5	1.02			

Berea128 data set

Berea128 sample data

3

Easting

Northing

Permeability

11.5	0.5	39.5	27.5	16.5	50	18.5	28.5	66
17.5	0.5	38	39.5	16.5	57	35.5	28.5	67
24.5	0.5	45.5	4.5	17.5	27	0.5	29.5	45
39.5	0.5	64.5	24.5	17.5	53	5.5	29.5	57
11.5	1.5	56	30.5	17.5	68.5	27.5	29.5	45
28.5	1.5	32.5	32.5	17.5	58	28.5	29.5	38
31.5	1.5	25	5.5	18.5	30	30.5	29.5	60.5
19.5	2.5	70	7.5	18.5	42	6.5	30.5	59
24.5	2.5	46.5	11.5	18.5	46	7.5	30.5	61
30.5	2.5	30.5	25.5	18.5	69	10.5	30.5	48.5
6.5	3.5	39.5	10.5	19.5	43	21.5	30.5	36
10.5	3.5	66	26.5	19.5	49.5	31.5	30.5	64
28.5	3.5	24	37.5	19.5	50	35.5	30.5	64
21.5	4.5	42	13.5	20.5	42	7.5	31.5	50
26.5	4.5	29	19.5	20.5	55	19.5	31.5	47
33.5	4.5	62	23.5	20.5	52	32.5	31.5	80
36.5	4.5	72.5	24.5	20.5	58.5	6.5	32.5	65.5
23.5	5.5	37.5	3.5	21.5	58	8.5	32.5	70
5.5	6.5	49.5	10.5	21.5	53	11.5	32.5	71
24.5	6.5	30	16.5	21.5	60	33.5	32.5	81
14.5	7.5	40	4.5	22.5	40	34.5	32.5	82
16.5	7.5	39.5	7.5	22.5	32	36.5	32.5	93.5
18.5	7.5	27	26.5	22.5	58	9.5	33.5	47
20.5	7.5	32.5	39.5	22.5	78	13.5	33.5	48
27.5	7.5	56	15.5	23.5	47	16.5	33.5	43
39.5	7.5	90.5	29.5	23.5	36	33.5	33.5	79
31.5	8.5	75	30.5	23.5	45	34.5	33.5	74.5
3.5	9.5	40	39.5	23.5	95	15.5	34.5	33.5
17.5	9.5	35.5	21.5	24.5	50	17.5	34.5	55
29.5	9.5	65	24.5	24.5	50	20.5	34.5	54.5
10.5	10.5	56	8.5	25.5	48	31.5	34.5	89
37.5	10.5	78.5	30.5	25.5	55	34.5	35.5	77
38.5	11.5	86.5	33.5	25.5	35	4.5	37.5	61
10.5	12.5	36	37.5	25.5	88.5	27.5	37.5	74
17.5	12.5	55	38.5	25.5	63	28.5	37.5	68
30.5	12.5	76.5	16.5	26.5	50	36.5	37.5	98
24.5	13.5	75	25.5	26.5	49	1.5	38.5	54
35.5	14.5	66	28.5	26.5	45	10.5	38.5	42.5
20.5	15.5	53	13.5	27.5	52	19.5	38.5	60
23.5	15.5	65	18.5	27.5	71	37.5	38.5	78.5
4.5	16.5	28	33.5	27.5	73	4.5	39.5	62
17.5	16.5	47	36.5	27.5	66	21.5	39.5	78
26.5	16.5	60	3.5	28.5	55			

APPENDIX B – Estimation of Average Grade Above the Highest Cut Off

In this appendix we derive Equations 2.45 and 2.46 giving the average grade of ore above the highest cut off. For convenience the notation has been changed slightly. Instead of using the cumbersome notation $F(A; z)$ to represent the cdf we will use instead $\phi(z)$ and we shall abbreviate $\phi(z_K)$ to ϕ_K .

The quantity of metal recovery factor q for ore with grade between z_K and z_{\max} is represented by the area of the shaded region in Figure B.1.a. The average grade \bar{z}_K is that grade in the interval $[z_K, z_{\max}]$ which makes the area of the rectangle with side lengths $(\phi_{\max} - \phi_K)$ and \bar{z}_K equal to the area representing q . This rectangle corresponds to the shaded region in Figure B.1.b. The value of \bar{z}_K can be found by equating the areas of the two shaded regions shown in Figure B.1.c. Therefore we need

$$\int_{z_K}^{\bar{z}_K} \left(1 - \frac{\lambda}{z^\omega}\right) dz - (\bar{z}_K - z_K) \phi_K = (z_{\max} - \bar{z}_K) \phi_{\max} - \int_{\bar{z}_K}^{z_{\max}} \left(1 - \frac{\lambda}{z^\omega}\right) dz$$

which may be rearranged to give

$$\bar{z}_K = \frac{\int_{z_K}^{z_{\max}} \left(1 - \frac{\lambda}{z^\omega}\right) dz + z_K \phi_K - z_{\max} \phi_{\max}}{(\phi_K - \phi_{\max})}$$

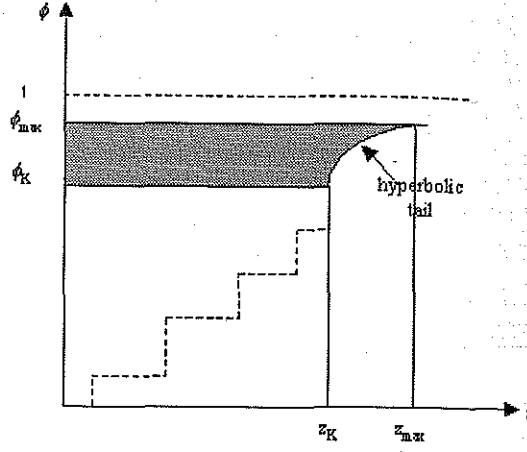


Figure B.1.a. Quantity of metal recovery factor for ore with grade above between z_K and z_{\max} .

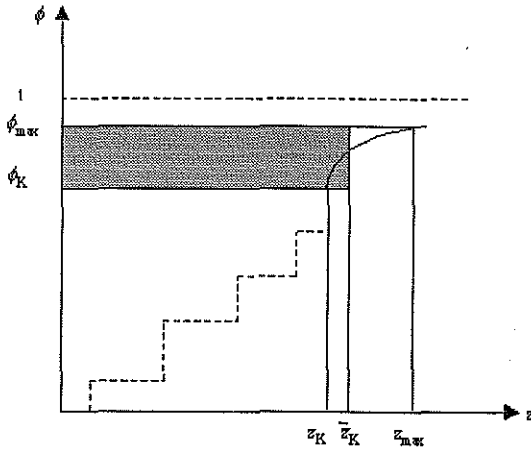


Figure B.1.b. Average grade between z_K and z_{\max} .

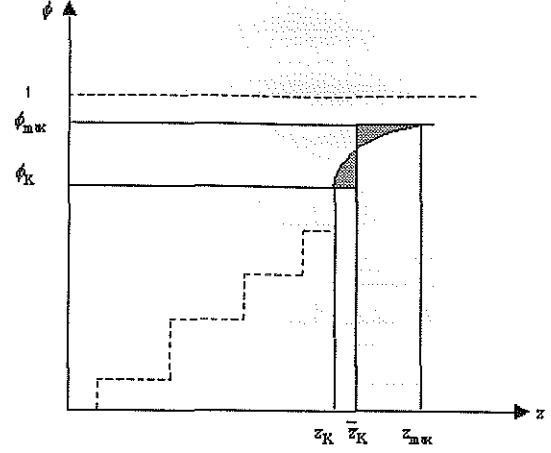


Figure B.1.c. Areas to be equated.

Noting that when $\omega > 1$

$$\begin{aligned}
 \int_{z_K}^{z_{\max}} \left(1 - \frac{\lambda}{z^\omega}\right) dz &= \left[z - \frac{\lambda}{1-\omega} z^{1-\omega} \right]_{z_K}^{z_{\max}} \\
 &= (z_{\max} - z_K) - \frac{\lambda}{1-\omega} (z_{\max}^{1-\omega} - z_K^{1-\omega}) \\
 \text{we find } \bar{z}_K &= \frac{(z_{\max} - z_K) - \frac{\lambda}{1-\omega} (z_{\max}^{1-\omega} - z_K^{1-\omega}) + z_K \phi_K - z_{\max} \phi_{\max}}{(\phi_K - \phi_{\max})}
 \end{aligned}$$

$$\begin{aligned}
&= \frac{z_{\max}(1-\phi_{\max}) - z_K(1-\phi_K) - \frac{\lambda}{1-\omega}(z_{\max}^{1-\omega} - z_K^{1-\omega})}{\phi_K - \phi_{\max}} \\
&= \frac{z_K(1-\phi_K) - z_{\max}(1-\phi_{\max}) + \frac{\lambda}{\omega-1}(z_K^{1-\omega} - z_{\max}^{1-\omega})}{\phi_{\max} - \phi_K}
\end{aligned}$$

which is equivalent to Equation 2.45.

When $\omega = 1$ we have

$$\begin{aligned}
\int_{z_K}^{z_{\max}} \left(1 - \frac{\lambda}{z^\omega}\right) dz &= \int_{z_K}^{z_{\max}} \left(1 - \frac{\lambda}{z}\right) dz \\
&= [z - \lambda \ln(z)]_{z_K}^{z_{\max}} \\
&= (z_{\max} - z_K) - \lambda(\ln(z_{\max}) - \ln(z_K))
\end{aligned}$$

This gives us $\bar{z}_K = \frac{(z_{\max} - z_K) - \lambda(\ln(z_{\max}) - \ln(z_K)) + z_K\phi_K - z_{\max}\phi_{\max}}{\phi_K - \phi_{\max}}$

$$\begin{aligned}
&= \frac{z_{\max}(1-\phi_{\max}) - z_K(1-\phi_K) - \lambda(\ln(z_{\max}) - \ln(z_K))}{(\phi_K - \phi_{\max})} \\
&= \frac{z_K(1-\phi_K) - z_{\max}(1-\phi_{\max}) + \lambda(\ln(z_{\max}) - \ln(z_K))}{(\phi_{\max} - \phi_K)}
\end{aligned}$$

which is equivalent to Equation 2.46.

APPENDIX C – GRADETON Fortran 77 Code

```

program gradeton

c INPUT/OUTPUT Parameters:
c
c datafl          the input data
c nc              number of cut-offs
c co(i),i=1,nc    the cut offs
c outfl           the output file for results
c xsiz ysiz zsiz  block dimensions
c sg              specific gravity
c omega           omega
c phimax          maximum cumulative probability
c phi             proportion below cut off
c avg             average grade above cut off
c tonns           tonnage at cut off
c
c
c parameter(MAXDAT=5000, EPSLON=0.00001, MV=10, MC=50)

real    vr(maxdat,MC),co(MC),phi(MC),tonns(MC),xsiz,ysiz,
+       zsiz,sg,var(MV),xloc(maxdat),zmax,
+       yloc(maxdat),q(MC),avg(MC),omega,phimax,lambda
character datafl*40,outfl*40,str*40
integer  nvari,nc,nc1
logical  testfl
data    lin/1/,lout/2/

c
c Get the name of the parameter file - try the default name if no input:
c
c   write(*,*) 'Which parameter file do you want to use?'
c   read (*,'(a40)') str
c   if(str(1:1).eq.' ')str='graton.par'
c   inquire(file=str,exist=testfl)
c   if(.not.testfl) then
c       write(*,*) 'ERROR - the parameter file does not exist,'
c       write(*,*) '      check for the file and try again '
c       stop
c   endif
c   open(lin,file=str,status='OLD')

c
c Find Start of Parameters:
c
c   1 read(lin,'(a40)',end=98) str
c     if(str(1:4).ne.'STAR') go to 1
c
c Read Input Parameters:

```

```

c
  read(lin,'(a40)',err=98) datafl
  write(*,*) ' data file:      ',datafl
  read(lin,*,err=98) nc
  write(*,*) ' number of cut offs: ',nc
      read(lin,*,err=98) (co(i),i=1,nc)
      write(*,*) 'cut offs:      ',(co(i),i=1,nc)
  read(lin,'(a40)',err=98) outfl
  write(*,*) ' output file:      ',outfl
  read(lin,*,err=98)  xsiz,ysiz,zsiz
  write(*,*) ' block dimensions:  ',xsiz,ysiz,zsiz
  read(lin,*,err=98)  sg
  write(*,*) ' specific gravity:   ',sg
  read(lin,*,err=98) omega
  write(*,*) ' omega:              ',omega
  read(lin,*,err=98) phimax
  close(lin)

c
c Check for error situation:
c
c
  inquire(file=datafl,exist=testfl)
  if(.not.testfl) then
    write(*,*) 'ERROR data file ',datafl,' does not exist!'
    stop
  endif

c
c The data file exists so open the file and read in the header and
c write a header on the output file:
c
  open(lin, file=datafl,status='OLD')
  open(lout,file=outfl, status='UNKNOWN')
  read(lin,'(a40)',err=99) str
  write(lout,'(a40)') str
  read(lin,*,err=99)  nvari
  do 6 i=1,nvari
    read(lin,'(a40)',err=99) str
6  continue
  str='Grade tonnage calcs.          '
  write(lout,'(a40)') str

c
c Read and write all the data until the end of the file:
c
  n=0
7  read(lin,*,end=8,err=99) xloc(n+1),yloc(n+1),(var(i),i=1,nc)
77  format(2f10.2,10f8.4)
  n=n+1
  do 88 i=1,nc
88  vr(n,i)=var(i)

```

```

        nk=n
        go to 7
8    close(lin)

c
c Calculate the tonnages above each cut off
c
    do 10 j=1,nc
        cuv=0
        do 9 i=1,nk
            cuv=cuv+vr(i,j)
9        continue
        write(*,*) cuv
        phi(j)=cuv/nk
        tonns(j)=xsiz*ysiz*zsiz*sg*(nk-cuv)
10    continue

c
c calculate lambda and zmax
c

    lambda=(co(nc)**omega)*(1.0-phi(nc))
    zmax=(lambda/(1.0-phimax))**(1.0/omega)
    write(*,*)'zmax = ',zmax

c
c calculate quantity of metal above the highest cut off
c

    if(omega.eq.1)then
        q(nc)=((1-phi(nc))/(phimax-phi(nc))) * (zmax*(phimax-1)-
+             co(nc)*(phi(nc)-1)+lambda*(log(zmax)-log(co(nc))))
        else
        q(nc)=(co(nc)*(1-phi(nc))-zmax*(1-phimax)+
+             (lambda/(omega-1))*(co(nc)**(1-omega)-zmax**(1-omega)))
+             *(1-phi(nc))/(phimax-phi(nc))
        endif

c
c calculate the quantity of metal above each cut off
c

    do 11 i=nc-1,1,-1
        q(i)=q(i+1)+(phi(i+1)-phi(i))*(co(i+1)+co(i))/2.0
11    continue

c
c calculate average grade for each cut off and write to output file
c

```

```

        do 12 i=1,nc
            avg(i)=q(i)/(1.0-phi(i))
12      write(lout,78) co(i),tonns(i),avg(i)
78      format(f10.4,f15.3,f15.4)
            close(lout)
            stop 'Successful finish'
c
c Error in an Input File Somewhere:
c
98      stop 'ERROR in parameter file!'
99      stop 'ERROR in data file!'
        end

```

APPENDIX D – Example Parameter Files

Example parameter file for GAMV3M

Parameters for GAMV3M

START OF PARAMETERS:

xlavar.dat

1 2 3

1 4

-1.0e21 1.0e21

goodalla.var

10

10.0

5.0

2

0.0 30 10.0 0.0 90.0 1.0

90.0 30 10.0 0.0 90.0 1.0

10

1 1 10 0.14

1 1 10 0.3

1 1 10 0.47

1 1 10 0.66

1 1 10 0.88

1 1 10 1.23

1 1 10 1.65

1 1 10 2.39

1 1 10 4.30

1 1 10 6.05

\data file

\column for x,y, z coordinates

\nvar: column numbers...

\tmin, tmax (trimming limits)

\output file for variograms

\nlag - the number of lags

\xlag - unit separation distance

\xtol- lag tolerance

\ndir - number of directions

\azm,atol,bandwh,dip,dtol,bandwd

\azm,atol,bandwh,dip,dtol,bandwd

\number of variograms

\tail, head, variogram type, cut off

\tail, head, variogram type, cut off

\tail, head, variogram type, cut off

\tail, head, variogram type, cut off

\tail, head, variogram type, cut off

\tail, head, variogram type, cut off

\tail, head, variogram type, cut off

\tail, head, variogram type, cut off

\tail, head, variogram type, cut off

\tail, head, variogram type, cut off

Example parameter file for IK3D

Parameters for IK3D

START OF PARAMETERS:

bereal28.dat	\data file
1 2 0 3	\column for x,y,z and variable
direct.ik	\direct indicator input (soft)
-1.0e21 1.0e21	\data trimming limits
ber2f10.dat	\output file of kriging results
2	\debugging level: 0,1,2,3
ber2f10.dbg	\output file for debugging
40 0.5 1.0	\nx,xmn,xsiz
40 0.5 1.0	\ny,ymn,ysiz
1 0 1.0	\nz,zmn,zsiz
4 10	\min, max data for kriging
20.0	\maximum search radius
0.0 0.0 0.0 1.0 1.0	\search: ang1,2,3,anis1,2
0	\max per octant (0-> not used)
0 55	\0=full IK, 1=Med IK (cutoff)
1	\0=SK, 1=OK
10	\number cutoffs
34.55 0.10 2 0.0	\cutoff, global cdf, nst, nugget
1 14.8 1.0	\ it, aa, cc
305 35 0 1 1	\ ang1,ang2,ang3,anis1,2
1 18.6 0.8	\ it, aa, cc
35 305 0 1000 1	\ ang1,ang2,ang3,anis1,2
40 0.20 2 0.0	\cutoff, global cdf, nst, nugget
1 20.0 1.0	\ it, aa, cc
305.0 35 0.0 1.0 1.0	\ ang1,ang2,ang3,anis1,2
1 5.8 0.6	\ it, aa, cc
35 305 0.0 1000 1.0	\ ang1,ang2,ang3,anis1,2
46.05 0.30 2 0.1	\cutoff, global cdf, nst, nugget
1 13.60 0.7	\ it, aa, cc
310.0 40.0 0.0 1.0 1.0	\ ang1,ang2,ang3,anis1,2
1 7.80 0.59	\ it, aa, cc
40.0 310.0 0.0 1000 1.0	\ ang1,ang2,ang3,anis1,2
50.0 0.40 2 0.4	\cutoff, global cdf, nst, nugget
1 12.8 0.44	\ it, aa, cc
310 40 0.0 1.0 1.0	\ ang1,ang2,ang3,anis1,2
1 8.20 0.37	\ it, aa, cc
40 310 0.0 1000 1.0	\ ang1,ang2,ang3,anis1,2
55.0 0.50 2 0.27	\cutoff, global cdf, nst, nugget
1 11.60 0.52	\ it, aa, cc
310.0 40.0 0.0 1.0 1.0	\ ang1,ang2,ang3,anis1,2
1 6.20 0.39	\ it, aa, cc
40.0 310.0 0.0 1000 1.0	\ ang1,ang2,ang3,anis1,2
58.6 0.60 2 0.2	\cutoff, global cdf, nst, nugget
1 18.8 0.68	\ it, aa, cc

```

310 40 0.0 1.0 1.0
1 7.4 0.51
40 310 0.0 1000 1.0
64.45 0.70 2 0.41
1 21.0 0.55
315.0 45 0.0 1.0 1.0
1 3.8 0.44
45 315 0.0 1000 1.0
70.0 0.80 2 0.33
1 12.96 0.6
325 55 0.0 1.0 1.0
1 12.31 0.71
55 325 0.0 1000 1.0
78.15 0.90 1 0.39
1 13.40 0.61
90.0 0.0 0.0 1.0 1.0
84.92 0.95 1 0.80
1 12.0 0.2
90.0 0.0 0.0 1.0 1.0

```

```

\ ang1,ang2,ang3,anis1,2
\ it, aa, cc
\ ang1,ang2,ang3,anis1,2
\cutoff, global cdf, nst, nugget
\ it, aa, cc
\ ang1,ang2,ang3,anis1,2
\ it, aa, cc
\ ang1,ang2,ang3,anis1,2
\cutoff, global cdf, nst, nugget
\ it, aa, cc
\ ang1,ang2,ang3,anis1,2
\ it, aa, cc
\ ang1,ang2,ang3,anis1,2
\cutoff, global cdf, nst, nugget
\ it, aa, cc
\ ang1,ang2,ang3,anis1,2
\cutoff, global cdf, nst, nugget
\ it, aa, cc
\ ang1,ang2,ang3,anis1,2

```

Example parameter file for POSTIK

Parameters for POSTIK

START OF PARAMETERS:

```

goodf.dat
goodfpik.dat
1 0.5
5
0.3 0.66 1.23 2.39 6.05
0 1 0.75
cluster.dat
3 0 -1.0 1.0e21
0.0 50.0
1 1.0
1 1.0
4 1.50
100

```

```

\input from IK3D
\output file
\output option, output parameter
\number of cutoffs
\the cutoffs
\volume support, type, varred
\global distribution
\ivr, iwt, tmin, tmax
\minimum and maximum Z value
\lower tail: option, parameter
\middle : option, parameter
\upper tail: option, parameter
\maximum discretization

```